Virginia Tech Aerospace Engineering Senior Design Project
Spring Semester Final Report
1 May, 2003

2002-2003 AE/ME Morphing Wing Design

Laura Arrison
Kevin Birocco
Chuck Gaylord
Brandon Herndon
Katie Manion
Mike Metheny

Contents

List of Figures

List of Tables

Chapter 1

Introduction

1.1 A Brief History of Morphing

The concept of a morphing aircraft design has been around since 1903 when the Wright brothers made their first flight. Morphing, from Webster's dictionary, can be defined as "to cause a change in shape" and has been attempted in the aircraft industry several times with ideas such as the AFTI/F-111 MAW and the F-14. True aircraft morphing could be described as a smooth change in physical shape that produces beneficial and desirable differences in the flight characteristics of an aircraft.

Throughout the history of the aircraft, airplanes have been designed for particular tasks. An aircraft's assignment is based on its performance and physical shape. Take for example a World War II bombing aircraft; although good at carrying large payloads great distances, they were unable to defend themselves adequately and required escorts of smaller, more agile fighters for protection. Today we have thousands of aircraft, each one being the best for its given assignment. What morphing can enable us to do is provide a mission adaptable aircraft suitable for many tasks, instead of being limited to a select few. It can also be used to enhance the characteristics of an aircraft that is already in use (such as the

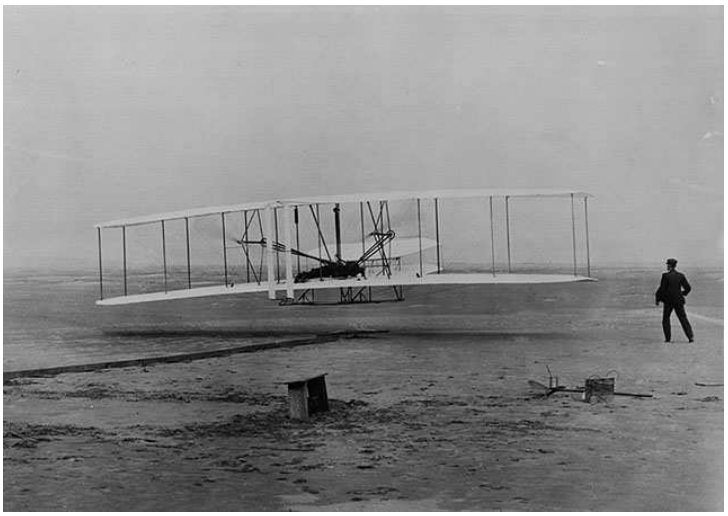

Figure 1.1: The Wright Flyer (http://www.nasm.edu/galleries/gal100/wrightflight.jpg)

F-18A with its active aeroelastic wing) and make it better at what it already does.

By changing the shape of the wing, the camber of the airfoil, or even the roughness of an aircraft's skin, the aircraft of the future will not be mission specific, but instead be able to adapt to many different situations and requirements. One can look at several designs and see how morphing is in use today and also see how far research has come and where it is looking to go in the future.

On December 17, 1903 the first aircraft flew in Kitty Hawk, North Carolina for twelve seconds and covered a distance of 120 feet[6]. This aircraft, called the Wright Flyer, used morphing to control its flight. To do this the Wright Brothers utilized a concept of morphing called wing warping. They used a variety of pulleys and cables to physically twist the wing to change the direction of the plane.

The Wright brothers came up with this revolutionary system by twisting an empty bicycle tube box with the ends removed[6]. By twisting the surface of each 'wing', they changed its orientation with respect to the oncoming wind. Such changes in position resulted in changes in the direction of flight. They tested their theory using a small kite, and later used this method to control the Wright Flyer.

1.2 Morphing in the Recent Past

Some modern designs of morphing aircraft can be seen in use today. These include the B-1B *Lancer*, the F-14 *Tomcat*, the AFTI/F-111 Mission Adaptive Wing, and the F/A-18A *Hornet* with Active Aeroelastic Wing (AAW). Both the B-1B and the F-14 use "swing-wing" technology so that the wing can have variable sweep. This is done primarily for supersonic aircraft, where swept wings are highly beneficial when travelling at high speeds. The AFTI/F-111 and the F/A-18A however create a seemless camber change to maneuver more quickly, achieve better lift to drag ratios, and to have greater ranges in flight.

1.2.1 B-1B *Lancer*

The B-1B officially went into operation on October 1, 1986. It has a blended wing-body configuration and can change its wingspan from a mere 78 feet to almost 140 feet by changing the sweep of its wing[7]. In the unswept position, the B-1B can take off in shorter distances and increase its range. In the swept position the B-1B can achieve speeds above the speed of sound. This can be used for high-speed penetration into hostile territory or to escape potential threats. The morphing aspect of this bomber has left it with several world records for speed, payload, and distance.

1.2.2 F-14 *Tomcat*

The F-14 *Tomcat* also utilizes swing wing technology much like the B-1B. It was designed to be an air-superiority fighter for the Navy. The swept wings of the F-14 play a slightly different role than the B-1B because the F-14 is a carrier based aircraft.

The variable swept wings are shoulder mounted and are programmed for automatic sweep during flight, although a manual override is available. The wing pivot structure spans the entire center of the airplane. IT is 22 feet wide, and is electron welded out of titanium[8].

Figure 1.2: B-1B *Lancer* (http://www.fas.org/nuke/guide/usa/bomber/b1-dvic162.jpg)

One drawback of this structure is that its enormous size greatly increases the weight of the plane.

The span of the airplane can increase from 38 feet to 64 feet in the unswept position. The normal sweep range for the wings is 20 to 68 degrees. It has an over-swept position of 75 degrees that allows for hangar storage within the carrier[8]. Not only does the morphing aspect help decrease storage space, but when completely unswept, it helps the F-14 take off and land in the short span of the carrier deck. When in the swept position the F-14 can reach velocities greater than twice the speed of sound. Both the F-14 and the B-1B use the swing wing to their advantage and are more versatile in their operations because of this morphing capability.

1.2.3 AFTI/F-111 Mission Adaptive Wing (MAW)

The AFTI/F-111 MAW is one of the first attempts at a smooth variable camber wing. This was a joint project between the United States Air Force (USAF) and National Aeronautics and Space Administration (NASA)[4]. The project called for a significant improvement in aircraft performance by adapting a plane's airfoil shape to each task required by the aircraft's

Figure 1.3: F-14 *Tomcat* (http://www.fas.org/man/dod-101/sys/ac/f-14-053.jpg)

mission. Their solution was a mission adaptive wing (MAW) that allows the leading edge of the wing to travel from +2 to -21 degrees and the trailing edge of the wing to travel from +4 to -22 degrees.

The MAW consists of variable camber leading and trailing edges, controlled by surface actuation linkages, and hydraulic servo systems driven by digital computers. For the camber variation each wing has three trailing edge and one leading edge segments. On the variable camber edges a flexible fiberglass skin is used to cover the wing. While the upper edge is smooth and continuous, the lower edge of the wing has overlapping tapered edges and sliding panels that can accommodate for the chord changes with camber variation. The pilot can choose either manual or automatic modes for the flight control of the wing. In both modes the outboard and midspan MAW trailing edge surfaces respond to roll stick inputs from the pilot to provide flap assistance for roll control[4].

The AFTI/F-111 MAW project proved to be successful. The aircraft performance was greatly enhanced with the variable camber wing. However, despite this apparent success, the MAW program faded out in the late 1980's.

Figure 1.4: AFTI/F-111 Mission Adaptive Wing

1.2.4 F/A-18A *Hornet* with Active Aeroelastic Wing (AAW)

One of the latest designs in morphing is an active aeroelastic wing (AAW), and can be found on an F/A-18A. In the past great measures have been taken to reduce twisting of wings and make them as stiff as possible. This in turn has made wing structures heavier and more rigid. Now designers are working, much as the Wright brothers did, to use the natural warping of the wing to control the aircraft, and in turn make it much lighter.

One of the reasons the F/A-18A was chosen for this project is that the pre-production wings that were put into storage were originally too flexible at high speeds. These wings were taken out of storage and used for the same trait that they were originally discarded for.

Figure 1.5: F/A-18A *Hornet* with Active Aeroelastic Wing

Researchers believe that AAW concepts will eventually evolve to control wing twist at high speeds and improve roll maneuvering, to the point that the use of a vertical tail may not be needed[10].

The amount of wing twist being considered for the F/A-18A is small (roughly 4 degrees maximum), but this turns out to be a large factor at high speeds. The payoffs for an AAW are large. Besides the major reduction in weight, the wing can reduce drag, increase range, and reduce fuel consumption. Again morphing has played a positive key role in aircraft development of today and the future.

1.3 Review of the 2001-2002 AE/ME Morphing Wing Designs

The 2002-2003 Morphing Wing Design Project is a continuation of the 2001-2002 Morphing Wing Design Project. It is meant to further develop last year's project and also to provide some new innovations. The 2001-2002 project goals included exploring different types of actuation on a wing, performing wind tunnel tests on the wings, and comparing their responses. Performing actual flight-testing was not a high priority for their project and was never completed. Information detailing their project and accomplishments can be found in their final report[5].

The 2001-2002 team experimented with three different types of actuation. These ideas included shape memory alloy actuation, piezoelectric actuation, and servo driven actuation. Problems arose in each of these designs in their respective final forms. The following subsections summarize these designs.

1.3.1 Shape Memory Alloy Actuation Design

The final model of the airplane using shape memory alloy actuation is shown as the top right wing in Figure 1.6. Shape memory alloys are materials that change shape when heated and return to their original shape when cooled. This system consists of a series of flexible ribs with wires made of shape memory alloys strung across the top and bottom in an antagonistic fashion. The ribs were cantilevered off the back of the plane and covered with foam creating the trailing portion of the wing. The wires were then heated which then produced work used to deflect the ribs and change the camber of the airplane wing. The wires gave a 15 degree deflection at 2% strain and a 30 degree deflection at 4% strain. To reverse the deflection of the tip, the wires on the other side become activated, however they could not deflect

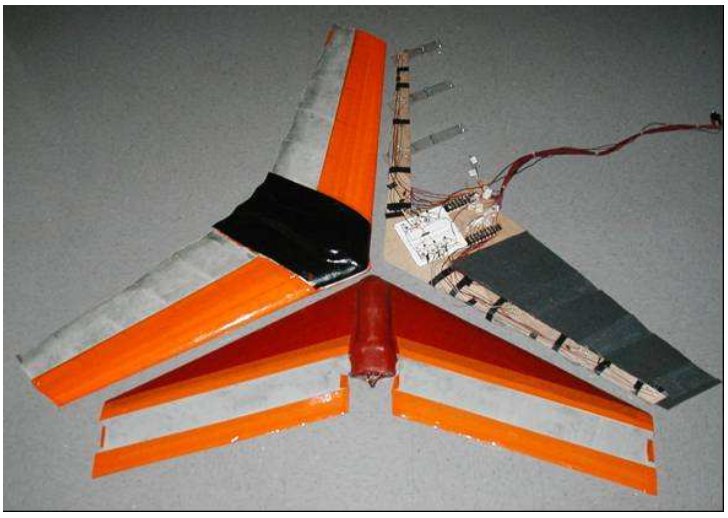

Figure 1.6: 2001-2002 morhping wing designs (left to right: servo actuated design, piezoelectric actuation design, shape memory alloy actuation design)

the surface until the passive wires are cooled. For this reason, some experimentation was conducted that studied the difference in responses between natural convection and forced convection. It was determined that when using forced convection the tip would return to its original position almost ten seconds faster than the same model being naturally cooled.

1.3.2 Piezoelectric Actuation Design

The final Piezoelectric Actuated model appears as the bottom middle wing of Figure 1.6. Piezoelectrics are similar to Shape Memory Alloys in that they deflect with the application of a stimulus. In piezos, the stimulus is an electric current. For a voltage range of -298 to 595 V, the system could generate a tip displacement in a range of -0.15 to 0.30 inches. A schematic of the deflections is shown in Figure 1.7. The piezoelectric system used sheets of the materials covered in foam and latex to create the trailing edge of the aircraft model. The wing used a joystick to operate a functional control scheme to deflect the trailing edge. A problem that arose with this system was a limitation in the amount of deflection of the trailing edge. In order for the small wing to maneuver well a deflection of more than one-

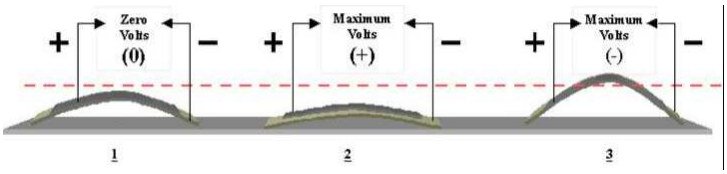

Figure 1.7: Deflection schematic of piezoelectric system

third of an inch is needed. Another problem is the high voltage required for the displacement of the trailing edge. The high voltage rapidly drains power sources.

1.3.3 Servo Actuation Design

The Servo Actuated model appears in the top left of Figure 1.6. This model utilizes ten ribs with two different sections. The first section uses a single servo and two different rib sections. The first rib section remains stationary while trailing rib section is deflected by the servo. This was used for the shorter portions of the trailing edge, near the wing tips. The second section consisted of two servos and three rib sections. In this system the two trailing rib sections moved according to servo deflection while the first remained stationary. This setup was used for the longer rib systems near the center of the wing. The structure of the trailing edge between the ribs was made of foam and the entire edge covered with latex. The biggest problem with this model was that the servos were not strong enough to stretch the latex skin.

1.4 2002-2003 AE/ME Morphing Wing Design

The 2002-2003 Morphing Wing project took the 2001-2002 project to the next level. The 2002-2003 team selected a Radio Controlled (RC) aircraft to instrument and fly. The team then designed, built, and flew an instrumented telescoping wing of similar planform and size. Flight test data was then extracted from both planes with the intent of comparing

the efficiency, maneuverability, and overall performance of the morphing aircraft to that of original RC aircraft. However, because similar flight plans were not developed for the two planes, it was difficult to make such comparisons and draw any solid conclusions. A goal then of the 2003-2004 team will therefore be to complete this objective.

The 2002-2003 project was more realistic than the 2001-2002 project in the sense that the goals were more focused; a single, telescoping wing aircraft was investigated. The 2001-2002 project dealt mainly with finding the best type of actuation system. While this is important, their project suffered because they never flew anything or collected any flight data. This is not to say that the 2001-2002 project was not important to the overall development of the ongoing Morphing Wing Design Project. Without the information gained by their experience, the 2002-2003 team would have had much more difficulty in foreseeing problems. This year's team attempted to pick up where the 2001-2002 team left off. Because of the accomplishments of the 2001-2002 team, the 2002-2003 team had some initial guidance. Since the least amount of problems occurred in the servo driven model, the 2002-2003 control morphing design planned on using the same type of actuation with some modification in servo power. However, due to difficulities in machining the various control morphing sections, the project was amended to a pure telescoping wing.

The following subsections discuss the 2002-2003 request for proposal (RFP), the project goals, and the mission drivers.

1.4.1 Request for Proposal (RFP)

This year, the design team was not assigned a request for proposal (RFP). Instead, an RFP was created to enhance and build upon the 2001-2002 design team's project. The 2002-2003 design team's RFP is to design a full flying delta wing with morphing capabilities to provide a comparison to a conventional full flying delta wing aircraft.

To accomplish the plan set forth by the RFP the first objective of the team was to

find a conventional radio controlled delta wing that was not too expensive, straightforward to build, and suitable for flying and instrumenting. Once the conventionally controlled RC plane was purchased, built, and instrumented, the team flew the delta wing and used the onboard instruments to obtain performance data. The next step was to design, build and fly a comparable morphing wing. Once this aircraft was flown and the same performance data recorded, the data sets could then be compared. Again, this final objective was not achieved but should be a primary driver for the continuing effort.

1.4.2 Project Goals

The first goal the team had set forth was to build upon what the 2001-2002 morphing team accomplished. The second and more important goal was to design, build, and actually fly a true morphing delta wing. The last goal the team had was to understand how the performance data from the conventionally controlled delta wing airplane and the morphing delta wing compared to one another. The team wanted to know what worked, what didn't work, and why.

1.4.3 Mission Drivers

The three primary drivers for the 2002-2003 team were feasibility, cost, and time. To meet the RFP everything the team did had to be feasible. The "far-fetched" ideas and designs that some people had were great for motivating the team, but in reality the final concept selected by the team had to be simple. The more complex the design, the more difficult it would be to meet the project goals and RFP. The team also decided to concentrate ideas to produce a minimum number of aircraft, probably one, possibly two. The final design for the morphing aircraft also had to be something that the team could actually build.

Cost was a concern because the team's budget was uncertain. There was no allotted

amount in the bank account that said how much was available to spend. If the team desires to raise money, concepts needed to be inventive and sponsors needed to be found.

To meet the goals, a close eye needed to be kept on time. Things were kept as simple and realistic as possible while still meeting the RFP. Time needed to be spent testing rather than debating about how to make things work the first time around. The bottom line for the 2002-2003 design team was to fly a morphing delta wing aircraft.

Chapter 2

Details of Morphing

2.1 Details of Morphing

In the most general case, a morphing aircraft is simply an aircraft which changes shape. However, as all aircraft change shape through use of control surfaces, a more specific definition that sets apart a "morphing" aircraft from a normal aircraft is needed. A morphing aircraft is one which has the capability to either seamlessly change part of its structure, or to drastically change its shape. This two-fold definition of morphing stems from the two primary drives for creating a morphing aircraft: control and mission performance.

2.1.1 Control Morphing

Today, most aircraft use discrete, hinged surfaces to control the aircraft. These surfaces can be quite sophisticated on large transport aircraft. Leading edge flaps are often combined with multiple trailing edge flaps that operate on a track to guide movement along a specified path. However intricate and elaborate these discrete control surfaces become, they are still compromises. Wings are typically optimized for some specific flight condition (usually cruise) and the ailerons, leading edge flaps, and trailing edge flaps are used to create camber

change for control or additional lift. The possibility of smoothly morphing the surface and shape of the wing itself, or "control morphing", offers many benefits. First and foremost are the performance enhancements possible with the operational flexibility of morphing. For example, when deflecting ailerons for a morphing wing, the degree of camber can be increased as the aileron traverses towards the wingtips, allowing for improved roll performance. A side benefit is the reduction of drag. As an example, the drag caused by deflection of flaps would be much higher than a wing designed to yield the same lift characteristics. For the same reasons, a controls-morphing aircraft would have lower trim drag. Discrete control surfaces are just that - discrete. They are limited spanwise and chordwise, taking up a finite area. The deflection needed by a discretely hinged elevator for trim would create more drag than a smooth, seamless change over the entire span and chord of the horizontal tail. Another benefit to control morphing is stealth. The B-2 *Spirit* has a split-flap system for yaw-control. When the split surface opens to control the B-2, this increases its radar signature. If an aircraft could morph for control, its stealth capabilities would be enhanced. One way a morphing aircraft could provide yaw stability without a vertical tail is by creating bumps / ridges on one wing, creating a drag differential.

2.1.2 Mission Morphing

The other type of morphing is mission morphing. Today, as in the past, the design of an aircraft is driven by the role which it will fulfill be it fighter, bomber, cargo, surveillance, etc. While the aircraft may eventually end up performing several duties in a variety of roles, it is usually optimized for one or two primary tasks. Using an aircraft in a role other than its primary one is inefficient, either from an operational costs perspective (fuel, maintenance), or from aircraft performance perspective (speed, maneuverability), or both. Additionally, the enormous cost and time investment in the development and production of a new aircraft makes it impossible to design and build many unique aircraft each optimized for different

missions; not to mention the logistics of having the right plane(s) in the right place at the right time. An aircraft with the capability of adapting its shape to optimize performance for different missions is the answer.

2.1.3 Proposals from DARPA: Morphing of Tomorrow

As revealed in Chapter 1, neither control morphing or mission morphing are new ideas. Both of these two types of morphing have been realized. One example of mission morphing is the F-14 *Tomcat* (Section 1.2.2), which has a swing-wing to help optimize flight at different speeds. An example of controls morphing is the F-111 Mission Adaptive Wing (MAW) project (Section 1.2.3), which gave the F-111 *Aardvark* morphing leading and trailing edges. What would be truly novel and unique is an aircraft that had capability for drastic, seamless, shape changes that could encompass both mission morphing and control morphing.

Along these lines, DARPA (Defense Advanced Research Projects Agency) is soliciting research proposals to realize such a concept. Announcement BAA 01-42, Addendum 7 details specifics of what DARPA is looking for: "Examples of specific controlled geometry changes include, but are not limited to, the following: 200% change in aspect ratio, a 50% change in wing area, a 5 degree change in wing twist, and a 20 degree change in wing sweep"[3]. Such a vehicle would most likely require significant advances in materials, but this is usually true of many advanced ideas; materials are often the 'limiting technology' in aerospace applications.

2.1.4 Problems with Morphing

An aircraft with such seamless morphing capability poses many problems not found in traditional aircraft. Materials are of course the major factor. For a mission morphing aircraft that does not utilize a hinged or telescoping design, not only must there be materials available to expand and contract while remaining taut, but there must also be clever internal struc-

ture capable of dynamically changing shape while maintaining a load-carrying ability. This added internal structural capability would most certainly add considerable complexity, and possibly weight. More complexity leads to more potential points of failure. In addition to materials issues, there are also power issues. While it may be aerodynamically more efficient to have a controls-morphing aircraft, the power required to maintain the wing or surface at a non-initial state may outweigh the aerodynamic benefits. These problems provide a unique area of research to seek new and innovative technologies to make the benefits of morphing worthwhile.

2.2 Morphing Design Concepts

The primary drive for this project is to design, build, and fly a morphing-capable remote controlled aircraft, and compare performance characteristics to a non-morphing aircraft of similar planform characteristics. Thus, the choice of the Delta Vortex (see Chapter 3) aircraft as our non-morphing comparison aircraft drove the general planform characteristics for our morphing vehicle. Since morphing is our priority, the majority of our preliminary design focus was on specific ways to morph rather than planform and sizing considerations. This phase of the design can be broken up into two areas: types of morphing to consider, and ways to achieve morphing.

2.2.1 Mission Morphing Consideration

What types of morphing could the team do? For mission morphing of a full-flying delta wing, one concept would be changing the leading edge sweep angle. The Delta Vortex model has a leading edge sweep angle of 42.2 degrees. If the team created an aircraft with a similar planform but had a variable sweep of say, 40 degrees to 60 degrees, this would also yield an aspect ratio and area change. This idea, however, was ruled out for several reasons. First,

it would require complex internal structure. The internal structure would have to be of a rib-spar construction, as a foam core would not work because foam cannot stretch. For the same reason, a hollow fiberglass shell would not work. Using ribs to guide the shape of the aircraft through such a change would be complex – the sweep angle change would require the ribs to change chord length, and to keep the airfoil profile similar, keeping the ribs oriented in the direction of the flow would be desired. A highly flexible skin that would stretch over the entire aircraft and yet still provide enough stiffness to keep the aircraft shape would also be required. For these reasons, such a concept was deemed to be unfeasible for the budget and time constraints of the project. A hinged swing-wing was not considered for two reasons: first, because a full flying delta wing combined with a swing wing would be of very limited benefit, and second, a swing-wing has been done before. Another option considered for mission morphing was a telescoping wing. A telescoping wing would allow for aspect ratio change and area change, but not require a highly flexible skin. It would, however, require a hollow primary structure to house the telescoping portion in its retracted position. For a full-scale aircraft, this could be problematic due to reduced volume for fuel storage.

2.2.2 Controls Morphing Consideration

In addition to mission morphing, the team also considered the possibility of controls morphing. On the tailless delta-wing aircraft comparison model, the Delta Vortex, the trailing edge of the aircraft contains elevons for pitch and roll control. An elevon is a combination of an aileron and an elevator, and each of the two control surfaces can be deflected independently. On the Delta Vortex model, there are also two vertical stabilizers with rudders attached. The team decided that the most benefit would be seen from a morphing structure that replaced the elevons. With this rough concept in mind, it was necessary to investigate the various methods of achieving such a design. The three concepts studied in-depth from last year were discussed by this year's team. The high voltage required for a piezo-electric solution,

combined with its inability to precisely maintain a deflected state, and the power required to maintain a non-equilibrium state made piezo-electric driven controls morphing undesirable for the team. The multiple second response of the temperature-driven shape-memory wires used last year make them unsuitable for our application, as it is desired to be able to fully deflect elevons in under a quarter of a second. The mechanical linkage, servo-driven solution seemed to be the most feasible approach. It does not require any exotic technologies, and mechanical linkages and hinging allow for greater predictability of the morphed structure shape. The difficulties of this sort of solution primarily involve finding a flexible skin to use over the underlying structure, and the onboard logic necessary to independently control several servos transparently based off of input from a standard remote control aircraft radio.

2.2.3 Three Initial Concepts

The team decided to attept both mission morphing and controls morphing. Ideas for mission morphing include a telescoping wing, a seamless span change, and a hinged wing. For controls morphing, the team planned to replace the elevons with a morphing structure. With these ideas in place, the next step was to come up with some initial geometry concepts that incorporated them, and then pick the best one. The requirement of the team's RFP to look at a full flying delta wing limited the scope of the team's planform choices. Three concepts were expanded upon and their merits and drawbacks debated by the team.

2.2.3.1 Blended Wing-Body with Telescoping Wing

The first concept depicted in Figure 2.1 is a blended wing-body concept with a telescoping wing. An advantage of this design is a span change of 65%, as well as ample interior space for instrumentation, as the telescoping portion is stored entirely in the wing portion of the blended wing-body. The disadvantages, however, are many. First, the complex, smoothly blended shape would be difficult to mold and construct. Second, the planform, while a

full flying delta wing, is not close in shape at all to the Delta Vortex, and performance comparisons would not be very valid.

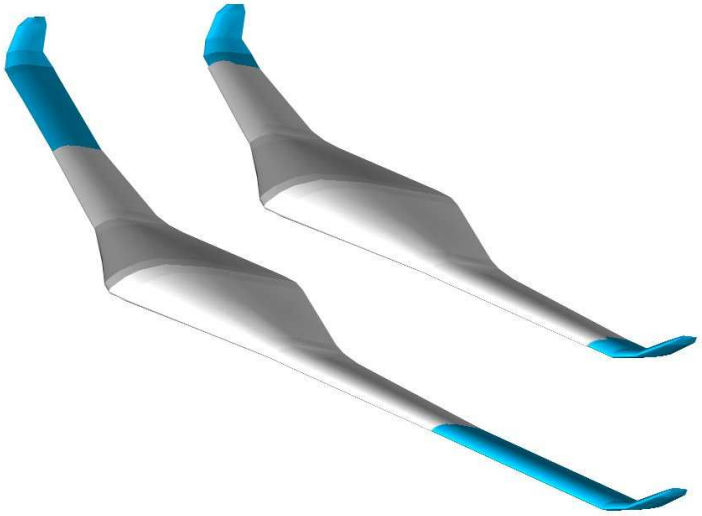

Figure 2.1: Blended wing-body concept

2.2.3.2 Delta Vortex Planform with Flexible Skin and Shifting Span

The second concept starts with the Delta Vortex planform, but moves the vertical tails to the wingtips, to prevent interference between the trailing edge and the attachment point and/or trailing edge of the vertical stabilizers.

This concept is not strictly telescoping, but involves a fully flexible skin, with the ribs of the airfoil moving outward along a track, increasing the span of the aircraft. This one-dimensioned scaling has the additional effect of changing the sweep of the aircraft. This concept is very attractive as it is a seamless mission morph, but unfortunately is impractical for our purposes. It was ruled out due to the complexity of a track system required for moving ribs differentially, and due to the requirements for a highly flexible skin that must cover the entire surface of the aircraft.

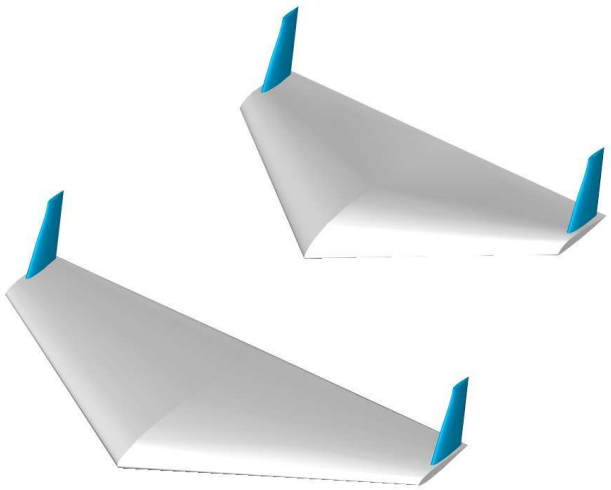

Figure 2.2: Delta Vortex planform with flexible skin and shifting span

2.2.3.3 Delta Vortex Planform with Telescoping Wing

The third concept considered again starts with the Delta Vortex planform, but removes the vertical tails and uses blended winglets for yaw stability.

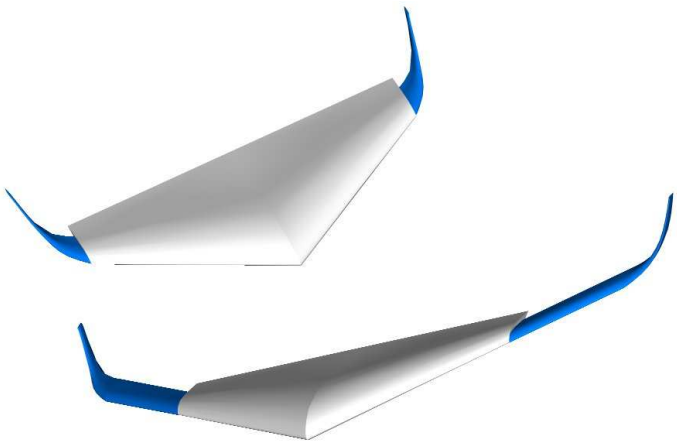

Figure 2.3: Delta Vortex planform with a telescoping wing

This concept requires a hollow shell to encompass the telescoping portion and a flexible trailing edge for controls morphing. This could be realized by constructing a fiberglass shell

for the vehicle, and using some sort of latex or rubber derivative for the trailing edge. A seamless joint could be achieved by laying an additional strip of fiberglass joining the two dissimilar materials. The design offers the capability of using the morphing trailing edge for control with the telescoping portion recessed, and additionally having ailerons present on the telescoping portion for quicker response with the telescoping portion fully extended. The telescoping wing would cause a CG shift, so a shifting mechanism would be required. In fact, the CG shifting mechanism could be used independently of the telescoping wing to change stability and performance characteristics while in flight. Use of a stability augmentation system (SAS) could be used instead of a CG shifting mechanism to balance the instability and provide increased maneuverability. That, however, is outside the scope of our project. This design is complex, but most importantly, it has flexibility. If, in experimental testing of morphing technology, it proves impossible to morph the trailing edge, conventional control surfaces can easily be implemented instead, and we will still possess a morphing aircraft by virtue of the telescoping portion. The converse is also true and although highly unlikely, it would be possible to morph the telescoping wing as well rather than using conventional ailerons, or twist the winglets to act as full flying rudders for yaw control. The flexibility of this design allows us to follow up on promising options, and be able to drop difficult or unfeasible solutions and still obtain a morphing aircraft we can build and fly.

2.2.4 Final Design

With the initial design for the morphing aircraft (named BetaMax) decided upon, the portion of the team responsible for its design branched off into two groups, one group working on mechanical actuation plans for morphing the trailing edge, and another group designing the actuation mechanism for the telescoping wing sections. As these concepts progressed, the aircraft design changed as well.

First, it was decided to use vertical tails almost identical to those on the Delta Vortex

instead of blended winglets on the telescoping portion. There were two major reasons for this. The first is to allow for better comparison between the two designs. Ideally, the only difference between the two aircraft should be the morphing capability. The second reason was due to complexity of creating a blended winglet. The team felt it would be easier to affix vertical tails and rudders to BetaMax in the same place they are on the Delta Vortex, and still not interfere with the morphing trailing edge.

The next design iteration removed 5.25 inches of span on each side of the BetaMax aircraft, for a total reduction in span from 54 inches to 43.5 inches. Due to the taper, this increases the tip chord from 12.5 inches to 17.5 inches. This was done to allow for a larger chord on the telescoping portion of the wing. Figure 2.4 below illustrates how this is achieved.

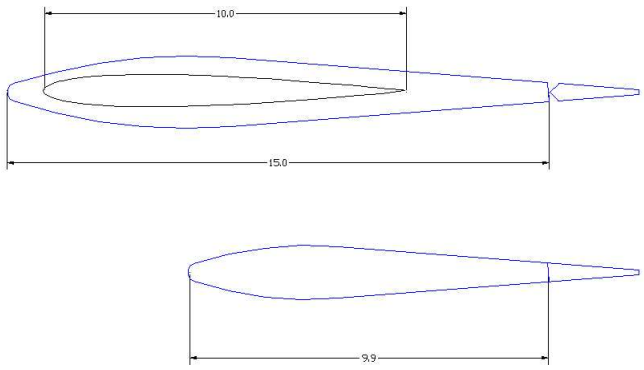

Figure 2.4: Tip chord comparison between the Delta Vortex and BetaMax

The lower portion of the figure shows the 12.5 inches tip chord rib of the Delta Vortex. As shown, only about 10 inches of chord is available for a telescoping wing, as the trailing edge section shown is reserved for elevons. Removing this rib and reducing the span yields the top portion of the figure, giving about 15 inches of available chordwise length to work with. However, some space is still needed for structure as well as servos to control the elevons. From this analysis, a telescoping wing with a 10 inch chord was decided upon.

The final and most significant design change was the decision to abandon controls morphing. The trailing edge morphing models that were designed and built (see Appendix B) were taking a great deal of time to construct and test, and seamlessly implementing a flexible skin added its own set of difficulties. This, compounded by problems with the laser cutter used to cut parts for the models drove the team to use conventional elevon controls and focus exclusively on the telescoping wing concept.

Since the morphing trailing edge was discarded, the team purchased an additional Delta Vortex kit, with the intention to build and modify it to include a telescoping wing. Sizing for the telescoping wing was determined from several factors. With the total span reduced to 43.5 inches, it was first decided that 5.25 inches of the telescoping wing would remain extended at all times, to yield the same span and almost the same area as the Delta Vortex. The internal length of the telescoping portion was limited by the interior volume needed for instrumentation, as well as the gearing system to extend and retract the wings. Chord length was limited by the new tip chord of 17.5 inches, rib thicknesses, and elevon placement. It was determined that the largest wing section we could extend would be a 10-inch chord and a 20-inch span.

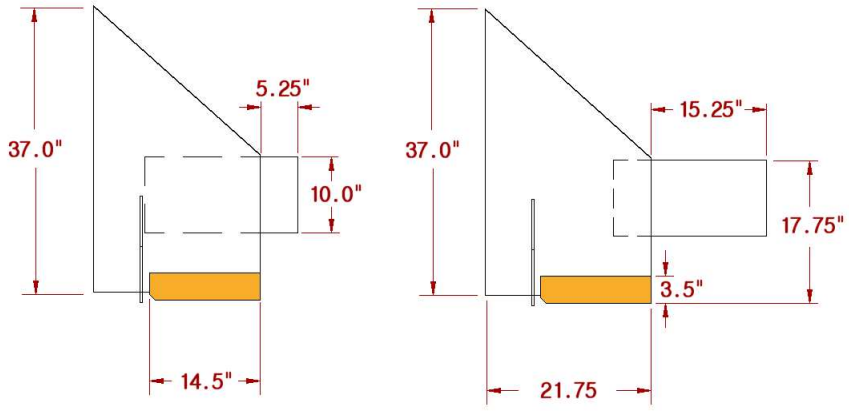

Figure 2.5: BetaMax dimensions with wings extended and retracted

For structural stability, when fully extended, 4.75 inches of the telescoping wing remains internal. Thus, BetaMax has a 54-inch span with wings retracted, and 74-inch span with wings fully extended, achieving a 36% increase in span and a 15% increase in area.

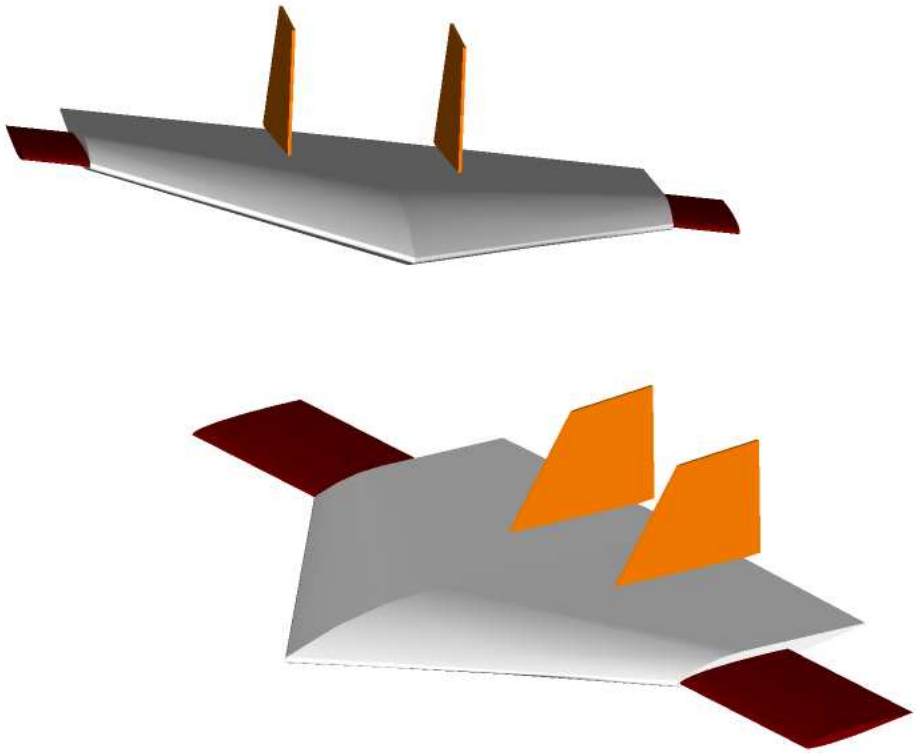

Figure 2.6: BetaMax in its final design configuration

2.3 Calculations

2.3.1 Range Improvement

The range equation for a propeller-driven aircraft flying at constant velocity is given below in equation 2.1. The constants γ_p and η_p relate to engine and propeller performance, and will be the same for the Delta Vortex and BetaMax. Thus, a range comparison reduces to

weight ratios and lift/drag ratios, as seen in Equation 2.2:

$$R = \frac{\eta_p}{\gamma_p} \frac{C_L}{C_D} \ln \frac{W_1}{W_2} \tag{2.1}$$

$$\frac{R_{BM}}{R_{DV}} = \frac{[(L/D)\ln(W_1/W_2)]_{BM}}{[(L/D)\ln(W_1/W_2)]_{DV}} \tag{2.2}$$

The Vortex Lattice method Tornado[1] was used to define the geometries of both aircraft and compute inviscid flow analyses. A reference flight condition of 45 mph at 2000 ft was chosen, and angle of attack (α) was adjusted until the Tornado output matched the C_L necessary for straight and level flight. Using the Tornado output of C_L and C_D, inviscid lift/drag ratios were calculated, see Table 2.1

Table 2.1: Cruise conditions parameters and results

	Delta Vortex	BetaMax retracted	BetaMax extended
Lift Coefficient, C_L	0.23	0.30	0.26
Lift-to-Drag, L/D	34.1	28.6	53.6
Angle-of-Attack (deg), α	4.3	5.6	3.6
Weight (lb), W	10.2	13.5	13.5
Planform Area (sq-in), S	1357	1367	1567
Span (in), b	54	54	74

The lift/drag ratios are quite high due to the nature of vortex lattice methods, however when used for comparison purposes they make a good first estimate of expected results. Plugging these numbers into equation 2.2 yields Equation 2.3:

$$\frac{R_{BM}}{R_{DV}} = \frac{53.6\ln(14.0/13.5)}{34.1\ln(10.7/10.2)} \tag{2.3}$$

Final calculations show a predicted 19% increase in range. If both aircraft weighed the same, this analysis predicts a 57% increase in range.

2.3.2 Wing Loading

Tornado also plots the span loading, which are included here for completeness. Tornado has the dimensional data for each aircraft, but weight is not an input, and the manual does not state how the program derives the span loading, so the units are in question, but the plots are valuable for comparison purposes.

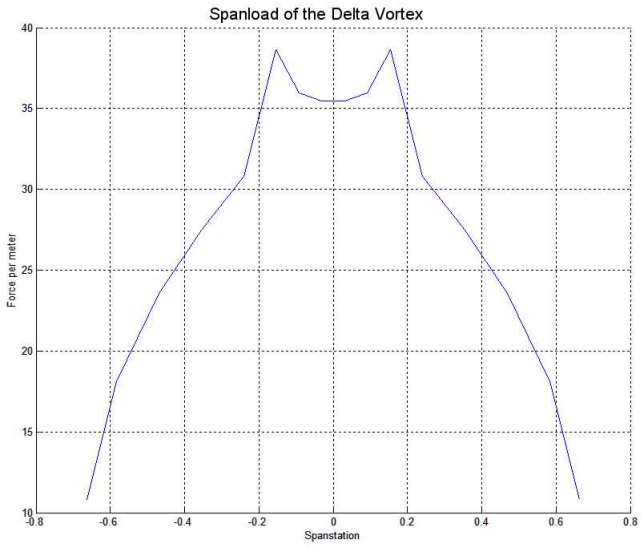

Figure 2.7: Tornado output of the Delta Vortex spanload

The span loading for the Delta Vortex (above in Figure 2.7) exhibits two peaks where the vertical tails are placed, and the loading drops slightly between the two vertical tails. This drop is not present in the span loading plots for both configurations of BetaMax (figures 2.8 and 2.9 below), and is most likely due to panel layout differences between the two models.

Notice that comparing all three spanload plots that BetaMax with wings retracted carries the heaviest spanload, followed by the Delta Vortex, and finally BetaMax with wings extended has the lightest span loading. With wings retracted, the peak spanload on BetaMax is 43% higher than with wings extended.

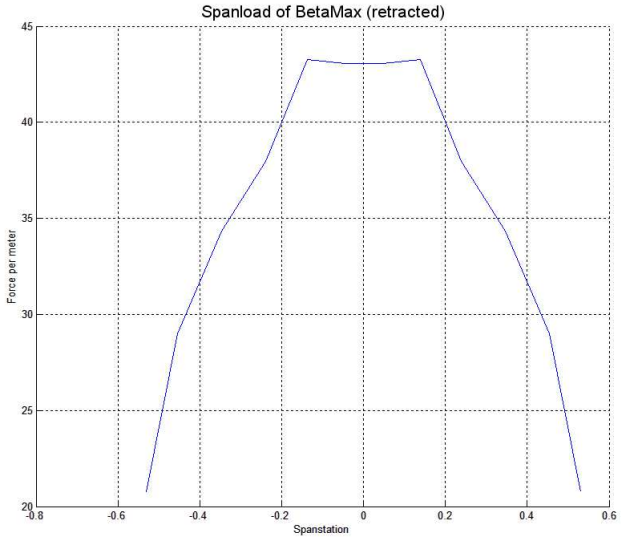

Figure 2.8: Tornado output of BetaMax spanload with wings retracted

2.3.3 Longitudinal Static Stability: Neutral Point and Static Margin Estimations

A primary goal of this project was to investigate the change in performance of a morphing aircraft over the conventional aircraft. To ensure an unbiased comparison, it was desired to have all other parameters to be as constant as possible. This was especially true for the longitudinal static stability.

In general, the longitudinal static stability is quantified by the aircraft's static margin, K_n, given by

$$K_n = h_n - h_{cg} \tag{2.4}$$

where h_{cg} and h_n are respectively the center of gravity and neutral points normalized with respect to the mean aerodynamic chord, $\bar{c}$. Since the Delta Vortex came as a kit with a proven flying history, the team was confident that the plane would fly with the manufacturer's recommended center of gravity location at $x_{cg} = 15$ inches aft of the apex. The objective then

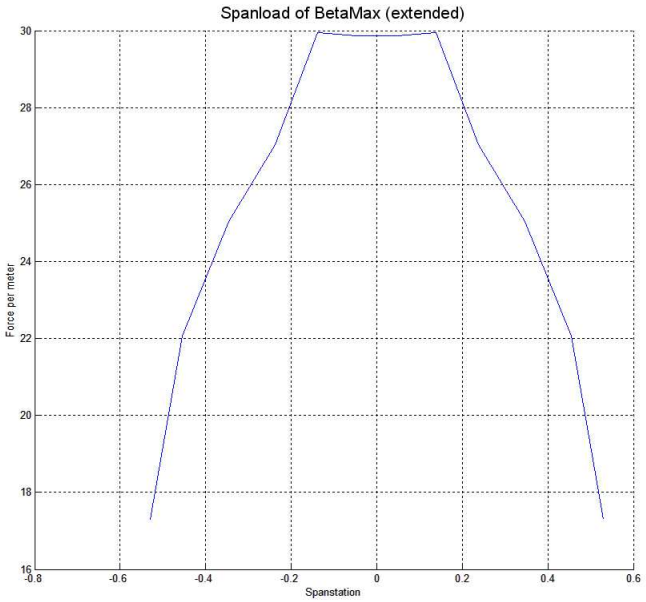

Figure 2.9: Tornado output of BetaMax spanload with wings extended

was to place the BetaMax's center of gravity such that it maintained the same static margin as the Delta Vortex. This indicated the need to determine the aircrafts' neutral points. It is important to note that the BetaMax's neutral point changed with the retraction and extension of the telescoping wings. Therefore, three neutral points were determined: that of Delta Vortex, that of the BetaMax with wings retracted, and that of the BetaMax with wings extended. It was assumed that the neutral point variation between the two extremes was linear.

To determine the neutral points, the Vortex Lattice Code VLM 4.997 was used. This gave the neutral point as a distance from the apex of the wing, x_n. Appendix C gives a sample code output with an explanation of the theory.

After determining the neutral points, the static margin of the Delta Vortex was calculated from Equation 2.4. Setting the static margins of the BetaMax planforms to that of the Delta Vortex gave the necessary BetaMax center of gravity locations. Table 2.2 summarizes the results and gives the final static margin as a percentage of $\bar{c}$. The nondimensional neutral

points were determined from

$$h_n = \frac{x_n - x}{\bar{c}} \tag{2.5}$$

where $x = 10.2$ inches is the distance from the apex of the wing to the leading edge of the mean aerodynamic chord. Similarly, the nondimensional center of gravity locations were determined from

$$h_{cg} = \frac{x_{cg} - x}{\bar{c}} \tag{2.6}$$

From Table 2.2, it is evident that some sort of center of gravity shifting mechanism would be necessary to maintain a constant static margin throughout all phases of the BetaMax flight. Unfortunately, due to project time constraints, the Delta Vortex static margin was maintained for the BetaMax extended case only. This cut the retracted BetaMax stability in half from 10% to approximately 5% of $\bar{c}$

Table 2.2: Neutral point and static margin comparison for Delta Vortex and BetaMax

Parameter	Delta Vortex	BetaMax retracted	BetaMax extended
neutral point (in), x_n	17.7 in	17.7 in	19.1 in
specified c.g. (in), x_{cg}	15 in	16.25	
static margin (in), $K_n\bar{c}$	2.70 in	1.45 in	2.85 in
mean aerodynamic chord (in), $\bar{c}$	24.8 in	27.1 in	26.1 in
static margin, K_n	0.109	0.055	0.109

Chapter 3

Aircraft Construction

3.1 Construction of the Delta Vortex: a Conventional Aircraft for Comparison

3.1.1 Plane Selection

For time saving purposes, it was decided to purchase the conventionally controlled aircraft in kit form. Before purchasing a kit, the team decided on the selection criteria. The first feature was the planform of the plane. This included the shape of the planform and also how the aircraft was made. The team decided on a delta wing, as specified by the RFP. Second, the team wanted the largest wingspan possible without making the plane too expensive or difficult to build. The larger the wingspan and over all area, the greater the Reynolds number and the closer one can get to resembling a real plane. The last features the team looked at were interior volume and power supply. Ample interior volume was needed for the instrumentation, and the team decided on a gas engine so the space and bulk of batteries would not be a consideration.

After investigating many delta wing options, the team narrowed down the choices to 5

possible planes. The top fives planes were chosen because they were the best representations of flying wings found. Table 3.1 below compares some of the specifications of the five planes.

Table 3.1: Plane Kit Selection FOM

Parameter	Wing Span (in)	Propulsion Type	Material
Shrike	43.5	gas	wood
Global B2	33.8	electric	plastic
Ripmax Delta Wing	45.7	gas	wood
Delta Vortex	54.0	gas	wood
Laser Arrow	39.4	gas	wood

Next, each plane was ranked based upon size (wingspan being the most important), type of power (gas or electric), material (foam, balsa, plastic), planform shape (how closely it resembled a delta wing), and finally interior volume for instrumentation. Size was considered to be most important, next was planform and volume, and finally fuel. Table 3.2 shows the figures of merit (FOM) for the plane kit selection. The winner was the Delta Vortex.

Table 3.2: Plane Kit Selection FOM

Parameter Weighting	Size 5	Fuel 2	Planform 4	Volume 4	Total
Shrike	4	4	2	3	48
Global B2	2	2	5	2	42
Ripmax Delta Wing	4	4	5	4	64
Delta Vortex	5	4	5	5	73
Laser Arrow	3	4	5	4	59

The Delta Vortex, made by Bruce Thorpe Engineering, has a span of 54 inches, overall length of 47 inches, a surface area of 1375 square inches, and weighs approximately 8 pounds without instruments. It is made primarily out of balsa wood, some hardwood for reinforcement, and the engine is powered by gasoline (Byron Glow Fuel, 10% Nitro and 20% Oil). It was purchased from ATS Radio Controlled Airplanes. Figure 3.1 is a picture of the completed Virginia Tech Delta Vortex in flight.

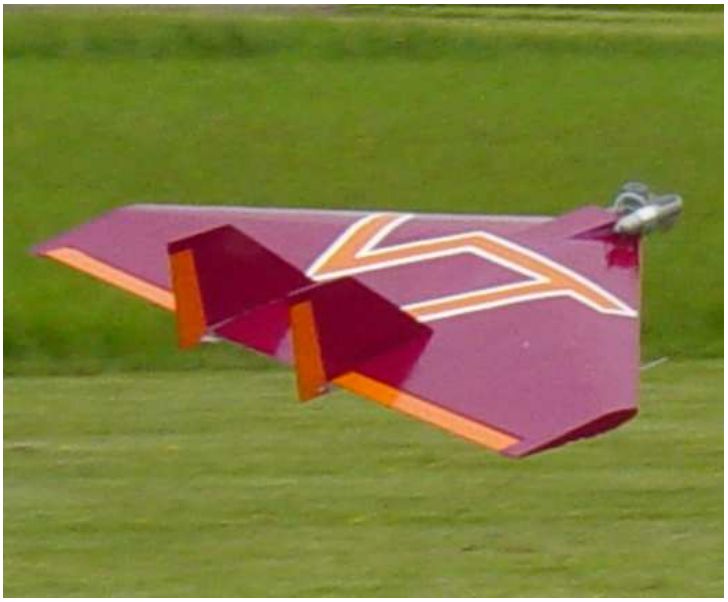

Figure 3.1: Delta Vortex in flight

Other materials such as epoxy, CA, wax paper, 6 servos, engine, engine mount, propeller, 16 oz. fuel tank, fuel line, three 3" wheels, three to four rolls of Monokote, and miscellaneous tools such as screw drivers and heat irons needed to build the plane had to be purchased elsewhere. The engine is an OS 0.91 FX with an output of 2.8bhp and a weight of 19.3oz (www.osengines.com/engines/osmg0591.html). The servos are HiTec programmable digital servos, model number HS-5645MG (www.hitecrcd.com). They use a 6V NiMh battery. The following companies were used to obtain the materials: Tower Hobbies, HeliHobby, and Techsburg.

3.1.2 Delta Vortex Construction

Once the kit and building supplies arrived, members of the team working on building went to work assembling the plane. There were directions provided, and with the exception of a few variations the team was able to follow them. The team began by cutting out the pieces of balsa wood that were not already cut out for us. Construction of the main structural

components of the plane was performed by putting together the ribs and the spars. The ribs were evenly spaced across the span except between the two middle ribs, which had some extra room between them. Once completed this space would be used for instrumentation and the fuel container. Balsa sheeting was used to overlay the ribs on the leading edges and mid-section, and thicker balsa was used for the trailing edge where the elevons were to be mounted. Mounts for the servos were made and placed between the ribs as specified by the directions, the fuel box was constructed, and the engine mount was attached to the nose. Figure 3.2 is a photograph of the Delta Vortex under construction.

Figure 3.2: Delta Vortex under construction

Next the original instrumentation bay design was modified to accommodate the desired instrumentation setup. The bay size was increased to make room for all the instruments, and the hatch was made larger for easy access to the inside of the plane. Instead of a small hatch right in the center of the plane, the design team expanded the hatch to entail almost the entire mid section of the plane. Holes were cut in a few of the ribs so all the instruments would fit, and mounts were made so that the instruments did not move around while in flight.

The vertical tails were preassembled, and holes were cut out towards the rear of the

middle section sheeting on the top side of the plane for them to fit into. Control horns were put onto the rudders and elevons for the actuator rod to attach and finally the plane was covered in MonoKote. Lastly, the landing gear, servos, engine, propeller, and control surfaces were installed. The photograph below in Figure 3.3 is the underside of the plane showing the instrumentation hatch, servos, and landing gear. Figure 3.4 is a photograph of the completed Delta Vortex following its fourth flight on April 19, 2003.

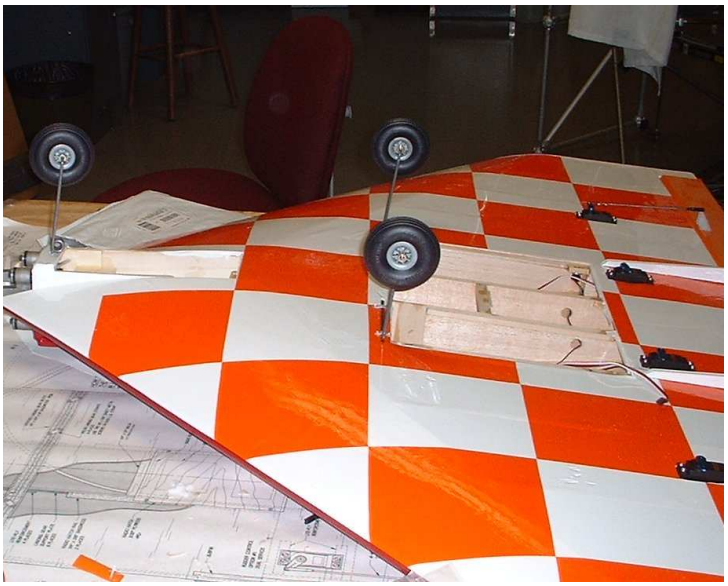

Figure 3.3: Lower surface of Delta Vortex with visible landing gear and instrumentation hatch

Before the instrumentation was installed, Delta Vortex had one test flight. This was a successful flight. After the Delta Vortex came back, the instrumentation process began. Details about the instrumentation selection, implementation, and testing can be found in Chapter 4. The data extracted during the ensuing flights is given in Chapter 5. The final instrumented and balanced plane weighed 10.2 lbs without fuel.

Figure 3.4: Completed Delta Vortex

3.2 Construction of the Beta Max: the 2002-2003 Morphing Aircraft

3.2.1 General Construction

After the decision was made to build the morphing aircraft with just the telescoping wing, the design team went ahead and purchased another Delta Vortex from Bruce Thorpe Engineering (BTE). The morphing aircraft, from here on out known as BetaMax, was built in much the same manner as the conventionally controlled Delta Vortex with only a few modifications.

The first major change came about in the size and design of the BetaMax planform. The area between the last two ribs was taken out of the design. This modification was done for two reasons. The first was so that the telescoping wing could have a larger chord. The second was due to the fact that the telescoping wing would not ever be fully retracted. To make sure that the initial planform area of BetaMax was as close as possible to the Delta

Vortex, the telescoping wing remained deployed from the end of the plane 5 inches with the wing fully retracted. This area will help make up for the area lost by taking out the last rib section. Figure 3.5 is a photograph of the two aircraft before their flight on April 19, 2003.

Figure 3.5: Delta Vortex (right) and BetaMax (left)

Once the main structure of the plane was put together without the last rib section, the telescoping wing had to be designed and built. The wing has a ten inch chord and is twenty inches long. It is made out of blue R7 insulation foam and covered with fiberglass. After the wing had been designed, holes were cut out in the balsa ribs of Beta Max for the telescoping wing to fit inside. After the wholes were cut and the wing was tested, the last rib was reinforced with 1/8th inch Lexan. Figure 3.6 shows the bottom side of Beta Max with the wings retracted and Figure 3.7 shows the bottom side of Beta Max with the wings extended.

With the telescoping wing taking up most of the internal volume in the sides of Beta Max, the servo mounts had to be moved closer to the rear of the aircraft so the servos would not interfere with the telescoping wing. In addition to moving the mounts, additional blocks had to be glued to the mounts so that the servo did not poke through on the topside of the airplane.

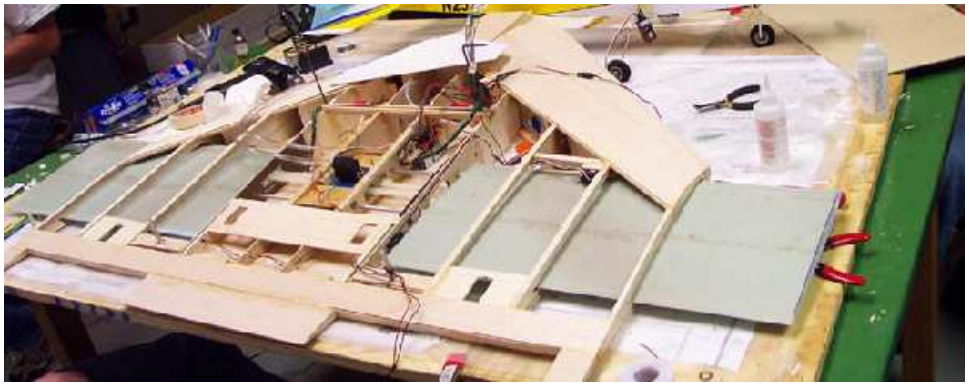

Figure 3.6: BetaMax with wings retracted

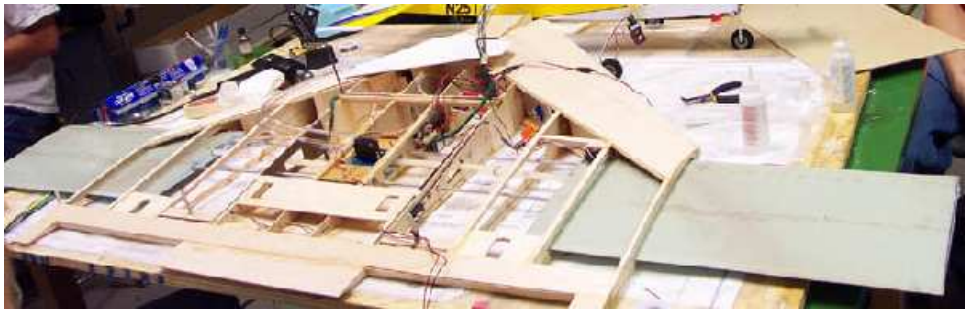

Figure 3.7: BetaMax with wings extended

The last change made to Beta Max, was the instruments were installed without a test flight occurring first. This decision was based upon lack of time, and trust that the pilot felt comfortable flying the new design without any trouble. The instrumentation process was the same for Beta Max as the Delta Vortex. There were minor changes in the location of instruments due to the telescoping wing, but the types and integration of the instruments remained the same.

Besides for the few changes mentioned above, the building process for Beta Max was the same as Delta Vortex. The plane was built, the wings were installed, the instruments were put in, and MonoKote was put on. Figure 3.8 is a photograph of the completed morphing plane Beta Max.

The plane used the same type of engine and fuel as the Delta Vortex and weighed 13.1

Figure 3.8: Completed BetaMax with wings fully retracted

pounds once completed. The next section discusses the mechanism used to deploy and retract the telescoping wing. Again, Chapter 4 will talk about the details of the instrumentation.

3.2.2 Telescoping Mechanism

The design of the mechanics of the telescoping wing was an interesting process. The benefits of the telescoping wing from an aerodynamic point of view were apparent, and mechanics behind implementing the extension of the wing were simple. However determining how to integrate the two designs within the structure of the Delta Vrtex kit was less than ordinary.

The aerodynamics and mechanics of the mechanism also had to agree. The chord length, thickness, and additional span of the airfoil were limited by the structure of the Delta Vortex kit which would be altered to allow for the telescoping wings. The length of the telescoping wing was limited by the original span of Delta Vortex kit. The allowable length of wing which could telescope was therefore not a consideration in increasing the area which would telescope. The length that would extend could only be as long as the half span of the Delta Vortex, minus room for instrumentation at the center rib. The chord length of the wing was mainly limited by the chord length of the exterior ribs, however it was further

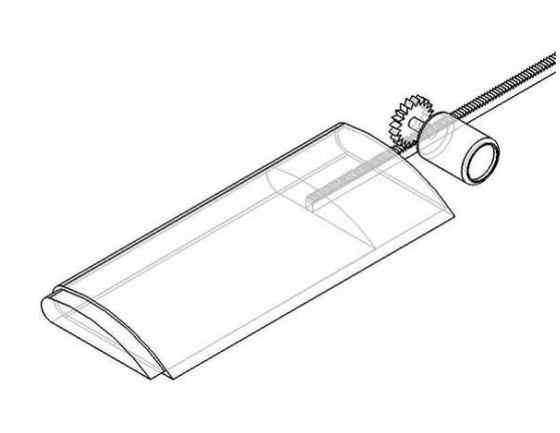

Figure 3.9: Rack and pinion device with wing retracted

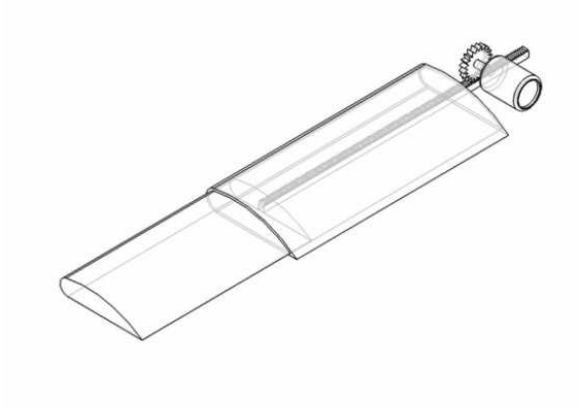

Figure 3.10: Rack and pinion device with wing extended

limited by the existence of the control surfaces on the trailing edge of the Delta Vortex. Since the purpose of the telescoping wing was to increase the aspect ratio of the delta wing by increasing the total planform area; and thus adding benefits in takeoff, landing and low speed cruise; maximizing the chord length of the telescoping wing was important. Because of these considerations the last rib on each side in the plans for the Delta Vortex was eliminated so that the chord length of the telescoping wing could be made longer. Having the telescoping wing extend from the second to last rib, allowed for a chord length of 10 inches, which is nearly 2 inches greater than if the last rib were intact. To account for the loss of span to the main fuselage of the aircraft, the telescoping wings were designed to retract no farther than

the original span of the Delta Vortex. Many designs were also considered on how to extend the wings. These included a spring-loaded design for quick extension, and many variations on the use of a rack and pinion gear system to slowly extend and retract the wings. The spring-loaded design would have been optimal since the time to extend would be minimized and the changes in aerodynamic effects would be immediate. However problems arose in determining how to retract the wings once the springs had released. There were also many chances for malfunction, and the extension could only be implemented once during flight. The rack and pinion system was determined to be the most reliable and efficient for the purpose. A schematic of the telescoping wing with the rack and pinion device can be seen in Figures 3.9 and 3.10.

The angle at which the wings would extend was the next design consideration. The original design called for the telescoping wings to extend at an angle equal to the leading edge sweep of the Delta Vortex. This design called for two separate rack and pinion devices, powered by two separate motors. Having two motors would also present potential problems. If one motor were to malfunction, only one wing would extend which would create extremely asymmetrical lift which would be detrimental in flight. Having two motors would also take up extras space and ass excess weight. The two rack and pinion design considerations are shown in Figures 3.11 and 3.12.

Because of these issues and the lack of interior space due to the existence of ribs, and installation of instrumentation, this design was altered so that the wings would extend with no sweep. Since this meant that the total angle between the lines of extension would be 180 degrees, two separate racks could be used with only one pinion powered by a single motor to extend both wings. One rack was mounted below the pinion and the other inverted above it. This saved space as well as ensured that the wings would move simultaneously. Custom acrylic housing was built and installed at the center rib of the plane to contain the device. The stop device was removed from the servo and a kill switch was mounted near on the

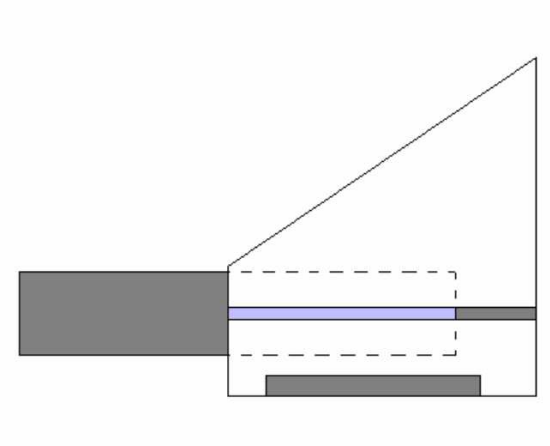

Figure 3.11: Wing extension without sweep

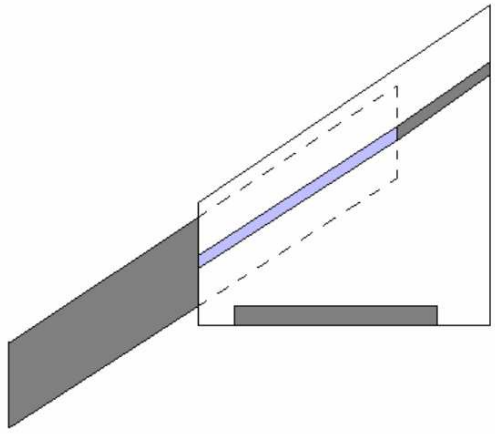

Figure 3.12: Wing extension with leading edge sweep

second to last exterior rib on the right side of the plane to ensure the ribs did not extend further than the designed distance of 10 inches in either direction. This double rack and single pinion design in shown below in Figure 3.13.

The rib sections of the Delta Vortex kit then needed to be altered to allow for the telescoping wings to be inserted. Each of the remaining exterior ribs was hollowed out in the shape of the new airfoil. Each telescoping wing was cut from R7 insulation foam using a symmetrical airfoil guide. Each wing was then coated in fiberglass and spray painted. Two guides were then inserted into each wing by drilling through the foam and inserting plastic

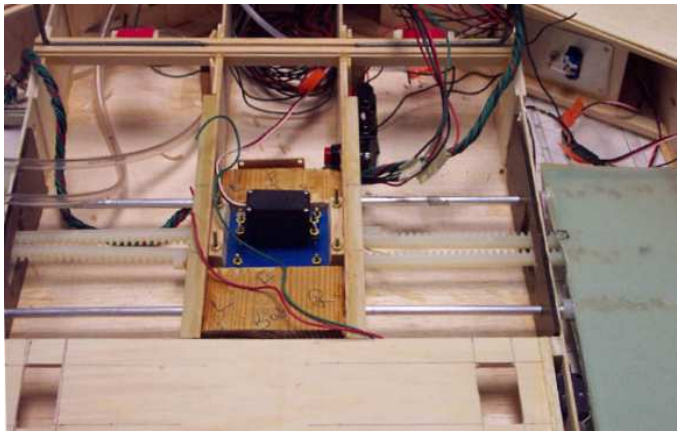

Figure 3.13: Double rack and single pinion design

tubing. Twin aluminum rails were mounted to on the interior ribs which ran through the plastic tubes, guiding and structurally supporting the wings during extension and retraction. . Each rack was mounted between the guides and extended the necessary length to allow for the designed extension and retraction. When the wings are retracted, the racks overlap each other and extend to the opposite side of the fuselage. The final design of the telescoping wing mechanism is shown in the photographs of Figures 3.6 and 3.7.

The final design of the telescoping wing was successfully installed and fully implemented during the first flight of the BetaMax. The single pinion with dual rack design proved successful in assuring equivalent extension and retraction on each side of the aircraft, while keeping the aerodynamic forces equal and controlled. Overall the design and mechanics of the telescoping wings were both successful and beneficial in accomplishing the preliminary goals of the system.

Chapter 4

Instrumentation and Signal Conditioning

As stated in Section 1.4, a primary goal of the 2002-2003 morphing wing design was to extract flight test data from both the BetaMax, the morphing aircraft, and the Delta Vortex, the conventional aircraft. To accomplish this task, both aircraft needed to be equipped with instruments to record trim/cruise and performance data. This chapter describes the quantities desired from the collected data, the instrumentation needed to collect that data, the final specifications on those instruments, and the process of their implementation including any necessary signal conditioning.

4.1 Desired Trim/Cruise and Performance Data

The quantities to be determined through flight tests of the two aircraft are as follows. Note that the list of instruments required to measure these quantities is given in Section 4.2.

Table 4.1: Quantities desired from flight test data

Trim/Cruise Data	Performance Data
airspeed control surface forces and positions	lift coefficient body rates accelerations

4.1.1 Rationale for Data Choice

The cruise and/or trim condition data includes the airspeed, and control surface positions. This data is useful both in generating an idea of what types of values to expect and in characterizing the aircraft's performance data.

Important performance data includes the lift coefficient, pitch and roll rates, and normal and axial acceleration. The following paragraphs detail the rational for determining these parameters. In general, these parameters were chosen because they will best represent the morphing wing's enhanced performance capabilities over the conventional aircraft.

The lift coefficient is an important parameter for all aircraft. Because of the increased span and greater aspect ratio of the telescoping wing, the morphing aircraaft will undoubtedly yield a higher lift coefficient.

It is important to note that the determination of the lift coefficient requires knowledge of all forces other than aerodynamic and gravitational forces. This includes, in particular, the value of the engine thrust at any given instant. This can be seen by looking at the equation needed to produce the lift coefficient from measured data. The equation for the lift coefficient is

$$C_L = \frac{Wn_n}{\bar{q}S}\cos\alpha + \frac{T + Wn_a}{\bar{q}S}\sin\alpha \tag{4.1}$$

where n_n and n_a are the normal and axial accelerations respectively in "g's", T is the engine thrust, W is the aircraft weight in lbs, $\bar{q}$ is the dynamic pressure, S is the wing planform

area, and α is the angle of attack. From this, it is clear that the lift coefficient depends on the thrust. Assuming small values for angle of attack the equation for the lift coefficient looks like this

$$C_L = \frac{W n_n}{\bar{q} S} \cos \alpha \tag{4.2}$$

In addition to forces and force coefficients, body rates as well as the linear accelerations themselves are also desirable information. In particular, the normal and axial accelerations, pitch rate, and roll rate are good measures of the aircraft agility in response to control inputs. For example, the roll rate would be useful when comparing the Delta Vortex roll maneuverability with the increased (hopefully) roll maneuverability of a differential camber (twist) morphing wing[9][10].

4.2 Instrumentation Needed

After careful consideration of the desired quantities listed in Table 4.1, a list of the necessary instrumentation was created. The list included a Pitot-static tube for dynamic pressure measurements (needed for airspeed and force coefficients), triaxial accelerometer (for accelerations and force coefficients), potentiometer (for control surface positions), strain gauges (for control surface forces), gyros or angular rate sensors (for body rates), an angle of attack vane (for angle of attack), and a GPS receiver (for position and altitude). Upon further consideration, the list was somewhat reduced to those quantities and necessary instrumentation shown in Table 4.2.

The GPS receiver and therefore the altitude measurement were deemed unnecessary because the Delta Vortex and the Morhping Wing aircraft would only be flying several hundred feet above the ground. The strain gauges were deemed unnecessary (for now at least) and control surface positions would be determined instead using the potentiometers.

Table 4.2: Actual quantities to be measured and their required instrumentation

Trim/Cruise and Performance Data	Required Instruments
airspeed	Pitot-static tube
control surface/throttle positions	potentiometers connected to the servos
lift coefficient	Pitot-static tube and accelerometer
body rates	gyros or angular rate sensors
accelerations	accelerometer

The angle of attack vane and therefore the angle of attack measurement were also deemed unnecessary under the small angle of attack assumption. That is, the force coefficients could be approximated fairly well by assuming a small angle of attack. Finally, the drag coefficient was dropped due to the difficulty in measuring the real-time thrust of the aircrafts.

It is important to note that in addition to instruments mentioned in Table 4.2, a data logger is also required to record the data for processing and reduction at a later time. A detailed description of this and the other instrumentation are given in the following sections.

4.2.1 Crossbow AD2000 Data Logger

The Crossbow AD2000 Data Logger depicted in Figure 4.1 was chosen over other models because of its multiple useful capabilities and it's overall compatibility with the other instrumentation. It has 8-channel capability meaning up to 8 different signals can be recorded simultaneously. In addition, the data logger is designed for spacecraft applications. It is therefore highly durable and capable of withstanding forces of several hundred gs. This is an important consideration when instrumenting aircraft that are still in the development stages (as with the morphing wing aircraft).

Other important features include a Lithium battery with 6-month maximum life, sampling frequency of 500 Hz for up to 99 min, data storage of up to 1 MB, and a download rate of 9600 to 115.2 Kbps. Additionally, the input voltage is from 0 to 5 V with a resolution of 20 mV. The Crossbow Data Logger has physical dimensions of 5.8 x 3.6 x 1.3 in and

Figure 4.1: Crossbow Data Logger

weights approximately 8 oz.

4.2.2 Dwyer Standard Model 1/8 Pitot-static Tube and Differential Pressure Transducer

The purpose of the Pitot-static tube is to measure the freestream dynamic pressure, $\bar{q}$, for calculating the aircraft relative airspeed, V, and lift coefficient, C_L. To determine the needed accuracy, an uncertainty analysis was performed on the airspeed and lift coefficient quantities as given in Appendix D. An acceptable, somewhat high-end error for the measured quantities was on the order of 5-10%. As an initial guess, a Pitot-static tube/pressure transducer error (and accelerometer error) was taken to be 5%. This gave an acceptable error result of 7.4% for C_L and 2.3% for V.

With collective error on the order of 2.1%, the Dwyer Standard Model 1/8 Pitot-static Tube and Differential Pressure Transducer combination shown in Figure 4.2 were well within this requirement. This in combination with their relatively low cost and small size made them a suitable choice for the dynamic pressure measurement. The 6-in long Pitot-

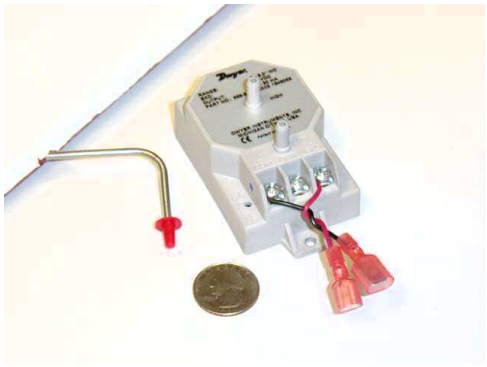

Figure 4.2: Dwyer Standard Model 1/8 Pitot Tube and Differential Pressure Transducer

static tube features a stainless steel tube with silver solder for leak-proof measurements. The differential pressure transducer attaches directly to the pitot-static tube and converts the dynamic pressure data into a voltage signal that can be read by the data logger. The pressure transducer needs at least 9 V to operate, reads up to 5 in of water, and has a response time of 15 msec. The physical dimensions are 2.5 x 1 x 2.8 in and it weighs 2.5 oz. The Pitot-static tube and transducer combination are best mounted on either wing of the aircraft well away from the wake of the engine propeller.

4.2.3 Crossbow CXL-10LP3 Triple Axis Accelerometer

As with the Pitot tube, an acceptable accelerometer error was determined in Appendix D to be on the order of 5%. The Crossbow CXL-10LP3 Triple Axis Accelerometer depicted in Figure 4.3 just fit the requirement at 5%. The primary reason for it's selection over comparable accelerometers was due to the generosity of Dr. Wayne Durham at Virginia Tech in loaning out his Crossbow accelerometer to the team.

The Crossbow Triple Axis Accelerometer features a measurement range of ± 10 g's and an output of 0 to 5 V. The physical dimensions are 1 x 1 x 1 in and the weight is approximately 1.5 oz.

Figure 4.3: Crossbow Triple Axis Accelerometer

4.2.4 Analog Devices ADXRS150EB/300EB Single Axis Angular Rate Sensor

Unlike the Pitot-static tube and accelerometer, the gyro was used to give direct data measurements only. An uncertainty analysis was therefore unnecessary. The primary problem in selecting a gryo or series of gyros (for multiple axes) was the relative cost. Most commercial gyros sell for more than $600.

An affordable solution was found in the way of the Hobbico Multi-Purpose Micro Piezo Gyro. These gyros are used to stabilize model aircraft and helicopters by measuring angular rates and adjusting the controls accordingly. The output given is a voltage linearly proportional to the angular rate. This seemed to be a viable option until it was found that the output signal (DC) could not be read by the data logger without a great deal of signal conditioning. Even then, problems would undoubtedly arise in calibration.

A second solution was the Analog Devices single axis angular rate sensor shown in Figure 4.4. These sensors were extremely small (7 x 7 x 3 mm) and very inexpensive. Originally, these sensors were available as free samples. Unfortunately, they came only as 32-pin BGA surface-mount package. Without the capability to solder directly to the

miniscule leads, this option was thought to be implausible. However, soon after difficulties arose with the Hobbico gyro, Analog Devices finished production of an 20-pin evaluation board containing the BGA circuit and the necessary capacitors needed to achieve the desired signal. This was the best choice at a mere $50 a piece. The angular rate sensor was available with two ranges: pm150 deg/s and pm300 deg/s. The 300 deg/s sensor was selected for measuring the aircraft roll rate while the 150 deg/s sensor was selected for the pitch rate.

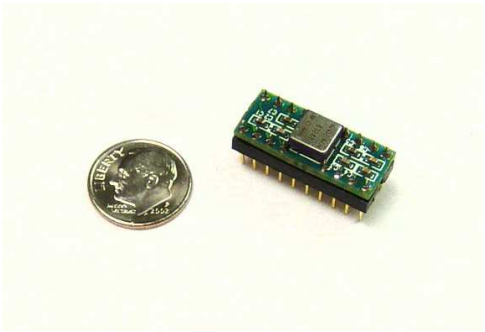

Figure 4.4: Analog Devices Single Axis Angular Rate Sensor

These angular rate sensors have an output range of 0 to 5 V. They require supply voltages of both 5 and 2.5 V. The physical dimensions are, again 7 x 7 x 3 mm for the BGA chip, and 1.0 x 0.4 x 0.5 in for the entire evaluation board. The total weight is 0.1 oz.

4.3 Instrument Implementation and Signal Conditioning

This section describes the signal conditioning needed to record meaningful flight test data. This signal conditioning includes the use of an independent power supply with voltage regulation, voltage dividers for potentiometers, low-pass filters for noisy accelerometers readings, and amplifiers for the angular rate sensors. Figure 4.5 shows the circuit board for the Delta Vortex. The BetaMax has a similar arrangement and produces nearly identical results.

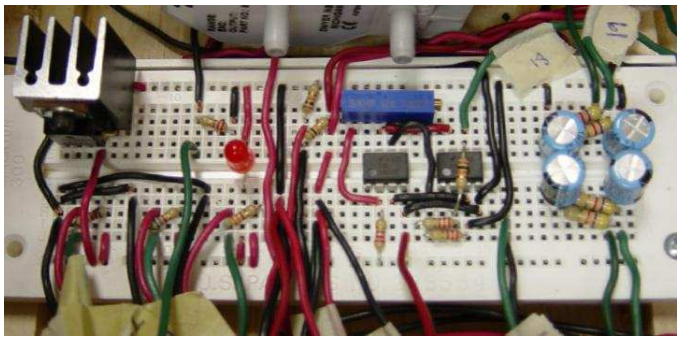

Figure 4.5: Signal Conditioning Circuit Board Mounted in the Delta Vortex

4.3.1 Power Sources for Instruments and Signal Conditioning

One of the key requirements for any instrumentation system is a constant power source. Because the Dwyer pressure transducer required a minimum of 9 V to operate, the data logger's 5-V supply voltage was insufficient by itself. A decision was therefore made to use two 9-V batteries connected in series to ensure a consistent power supply above the 9-V lower constraint. The data logger was used as a power source only for the accelerometer and Angular Rate Sensor as both specified the need for 5 and/or 2.5 V.

The two 9-V batteries, connected in series, yielded an 18-V supply. Of course, this value was subject to decay over time. To account for this, a voltage regulator was installed to provide a consistent, 12-V supply. This voltage regulator can be seen in Figure 4.5 with an attached heat sink. As long as the two 9-V batteries kept the minimum combined output over 12 V, the system would have a constant power source. After the circuit was implemented, the voltage regulator was shown to give a reading close to 11.85 V due to variation in the hardware.

Eventually, a third 9-V battery was installed in series with the initial two to give a negative voltage source with the same common ground. This negative voltage source was used to power the amplifier circuit also shown in Figure 4.5 used for the pitch rate Angular Rate Sensor. The amplifier circuit is discussed in detail in Section 4.3.5.

For convenience, the batteries were connected to a three-source swivel switch. This prevented the need to unplug wires when the board wasn't being calibrated or tested. Additionally, an LED was placed on the board to indicate when power was being supplied to the circuit.

4.3.2 Control Surface and Throttle Position Using Ballast Circuits

Initially, it was thought that the servo positions and therefore the control surface and throttle positions could be measured by monitoring the input to the servos from the radio receiver. Unfortunately, it was soon learned that this method would have to destroy the duty-cycle of the signal to convert it into a voltage readable by the data logger. There would also be a slight lag in the information became a fairly large (1mF) capacitance would be needed to smooth out the square wave input with which the the servos are controlled.

A second, a perhaps more standard method was soon adopted in which a 5 kΩ linear dial potentiometer was connected to the servos and/or the surfaces themselves. A sample of the Delta Vortex configuration is shown in Figure 4.6. The Beta Max used a surface-to-potentiometer mount to allow necessary space for the stowed telescoping wing.

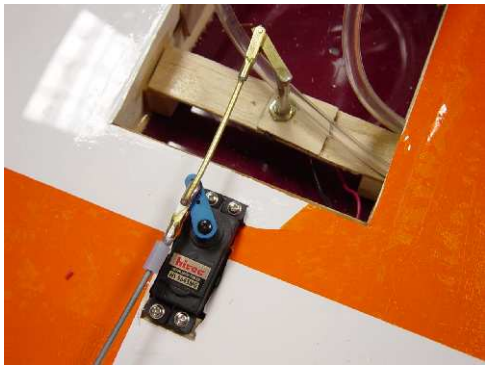

Figure 4.6: Connected Potentiometer and Servo for the Left Elevon of the Delta Vortex

To extract a voltage proportional to the position, each potentiometer was placed within a ballast circuit with another resistor and the constant 12 V power supply. For the

control surfaces, the potentiometer, at extreme deflections, yielded 160 deg of rotation. The throttle at its extremes reached nearly 90 deg. Taking these extremes into consideration, the potentiometers were positioned so they would turn from 20 Ω up to about 1.5 kΩ for the throttle and 2.7 kΩ for the control surfaces. The 20-Ω lower limit was assumed to ensure the potentiometer was never in the dead zone. Placing these potentiometers in the ballast circuit with the proper amount of resistance allowed the 12 V supply to be divided such that it would remain within the 0 to 5 V output range of the data logger. In an attempt to make the output range as closed to the extremes as possible, a 6.8-kΩ resistor was used for the control surfaces. Similarly, a 3.3-kΩ resistor was used for the throttle. All three ballast circuits can be seen in Figure 4.5.

4.3.3 Mounting the Pitot-static Tube and Differential Pressure Transducer

The first instrument the team configured and mounted was the differential pressure transducer and the Pitot-static tube. Together these instruments were used to determine the aircraft airspeed. The Pitot-static tube was mounted on the left side of the aircraft using epoxy. The two ports where connected to the two ports on the pressure transducer using 0.25 in diameter tubing. The pressure transducer, shown just above the circuit board in Figure 4.5, was mounted using two screws.

The pressure transducer allows between 4 and 24 mA to pass through it. This amperage in turn is directly proportional to the differential pressure between the ports of the Pitot-static tube. For this particular configuration, 4 and 24 mA corresponded to 0 and 5 inches of water respectively.

To condition the pressure transducer signal for sampling, a circuit was created using the constant, 12-V power source and a single, 220-Ohm resistor. Setting a data logger analog

input to read across the resistor yielded an output voltage of 0.88 V for 4 mA or 0 inches of water and an output voltage of 5.28 V for 24 mA or 5 inches of water. Since the data logger can read a maximum of 5 V, this indicated the resulting maximum pressure reading to be slightly lower than 5 inches of water. This was acceptable as the plane was expected to fly at speeds lower than those given by 5 inches of water (134 ft/s at sea level). A lower value resistor could have been used; however, this would have decreased the voltage sensitivity thereby decreasing the accuracy of the reading. Instead, the slight loss of maximum pressure reading was deemed acceptable to ensure a more accurate signal (on the order 0.02 inches of water with the data logger 20 mV resolution).

4.3.4 Mounting the Accelerometer and Conditioning with Low-Pass Filters

The Crossbow triple axis accelerometer was mounted at the center of gravity of the aircraft to prevent influences from the aircraft angular rates. It was mounted using foam and velcro. The data logger, since it is a Crossbow product as well, came pre-configured for use with the accelerometer. The accelerometer came with a five-port plug, one for ground, one for a positive +5 V input, and an output for each of the three axes. It is important to note that the +5 V lead was provided directly from the data logger and not the constant 12 V source.

Initially it was believed that no signal conditioning was necessary for this instrument. However, the first set of flight test showed frequency modulation indicated the presence of an aliased signal. This indicated that the sampling frequency (20 Hz) wasn't capturing the entire signal. It was later determined that this was the result of the engine vibration whose frequency of oscillation peaked around 200 Hz. Two solutions to this problem were presented: either sample at twice the highest frequency (namely 400 Hz) and post-process the signal or filter out the unwanted vibrations prior to sampling. Because of the limited memory on the

data logger, it was decided to keep the 20-Hz sampling frequency and filter the acceleration signals using RC low-pass filters. Second order RC circuits were chosen to accomplish this task. Capacitors of 100 μF and resistors of 4.7 kΩ were used giving an RC time constant of 0.47 seconds. This in turn resulted in a low-pass filter with a cutoff frequency of 2.1 Hz and 40 dB/decade attenuation. Two of these filters are shown in Figure 4.5. It is important to note that a third filter was not implemented as the lateral acceleration measurement was replaced by a pitch rate measurement.

4.3.5 Mounting the Angular Rate Sensors with Signal Amplification

Two of the Analog Devices single-axis gyros were used to give the roll rate and pitch rate of the two aircraft. A 300 deg/s gyro was used for the roll rate while a 150 deg/s gyro was used for the pitch rate. Rather than solder right to the gyro evaluation board, a separate circuit board was created for each gyro as shown in Figure 4.7.

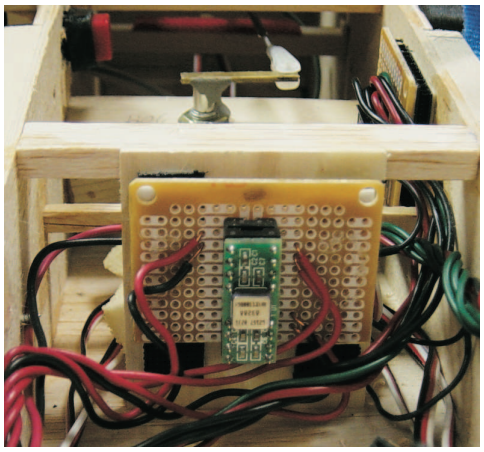

Figure 4.7: Angular Rate Sensor Mounted on a Circuit Board

Because it is not uncommon to have aircraft roll rates between 200 and 300 deg/s, the roll rate $\pm$300 deg/s gyro was adequate without signal conditioning. On the other hand,

it is highly unlikely that the pitch rate of any aircraft would exceed 30 to 40 deg/s in either direction baring some sort of longitudinal instability. The 150 deg/s gyro was then somewhat inadequate for the intended measurement. This particular range gave an accuracy of only 1.5 deg/s with the 20 mV resolution of the data logger. Because of this, it was decided that the signal needed to be amplified to give the desired range (between ±30 and ±40 deg/s). This would effectively increase the accuracy to 0.2 deg/s, a much more acceptable value for this application.

To accomplish this task, a dual op amp circuit with a linear taper potentiometer was implemented. A single op amp circuit was inappropriate as the Analog Devices' gyros output 2.5 V at 0 deg/s. This indicated that any amplification beyond 2 would yield the maximum 5-V output before the aircraft moved at all. Instead, a dual op amp configuration was used. The first op amp circuit inverted and reduced the constant 12-V power supply to -3.0 V using a linear taper potentiometer in place of the second resistor to fine tune the gain. The second op amp circuit then inverted and amplified the sum of this constant signal and that of the pitch rate gyro. Using an amplification close to 5, the resulting amplified signal gave a value near 30 deg/s at 5 V, 0 deg/s at 2.5 tab:cruise, and -30 deg/s at 0 V. This gave the desired ±30 deg/s range with an accuracy close to 0.2 deg/s.

4.4 Instrument Calibration

Instrument calibration was performed one of two ways. The first and easiest method of calibration was done using the manufacturer specifications. A second and more preferred method of calibration consisted of measuring two voltages corresponding to two distinct quantities. This latter method allowed for proper verification of the specified numbers. Unfortunately, not all of the instruments could be calibrated in this fashion. These instruments included the pressure transducer and the angular rate sensors.

In both cases, the instrument calibration led to two quantities: the slope (Units/V) and intercept (Units). The resulting values for each instrument are given in Table 4.3. The sign switch of the angular rate sensor factors between the two planes was due to the fact that the sensor axis was flipped in both cases. In both cases, positive roll rate is given as right-wing-down and positive pitch rate is given as nose-up. Other sign conventions adopted are positive-forward for axial acceleration, positive-up for normal acceleration, and positive-trailing-edge-down for the elevons.

Table 4.3: Slope and Intercept Parameters for Instrument Calibration (Volts to Desired Units)

Instrument	Delta Vortex		BetaMax	
	Slope	Intercept	Slope	Intercept
Roll Rate Sensor (deg/s)	200	-500	-200	500
Pitch Rate Sensor (deg/s)	18.67	-46.67	19.67	-49.16
Axial Acceleration (g)	-2.01	4.92	-2.01	4.92
Normal Acceleration (g)	2.01	-4.92	2.01	-4.92
Pressure Transducer (psf)	7.354	-6.346	7.354	-6.346
Throttle Potentiometer (%)	0.455	-0.125	0.251	-0.0689
Right Elevon Potentiometer (deg)	14.29	-17.14	13.16	-25.66
Left Elevon Potentiometer (deg)	-17.86	31.61	-14.08	31.83

4.4.1 Angular Rate Sensor Calibration

The angular rate sensors proved to be particularly difficult to calibrate. There was no available tool with which to spin the sensors at a known rate. Because of this, the Analog Devices factors were used without verification. This indicated the introduction of error associated with inaccurate manufacturer calibration. It was therefore decided to assume a conservative 5% error on the recorded values. This equated to errors of ± 15 deg/s error for the ± 300 deg/s sensor and ± 7.5 deg/s error for the ± 150 deg/s sensor. As it turned out, this was acceptable error for initial data collection as the roll rate sensor reached rates

of ±300 deg/s while the pitch rate sensor exceeded rates of ±50 deg/s. If and when these instruments are used for comparing the performance of the two planes, proper calibration will be necessary. The slopes for these sensors were given in deg/s/Volt while the intercepts were given in deg/s.

4.4.2 Accelerometer Calibration

Calibration of the accelerometer involved aligning a given axis with the gravity vector and recording the corresponding voltages. For the case in which the axis pointed up, a voltage was recorded corresponding to -1 g. Similarly, for the case in which the axis was pointed down, a voltage was recorded corresponding to +1 g. From these points, the slopes (g/Volt) and intercepts (g) necessary for calibration were recorded. Minimal error was assumed to be on the order of ±0.05 g. This was entirely due to the limited resolution of the data logger (20 mV).

4.4.3 Pressure Transducer Calibration

Like the angular rate sensors, the Pitot-static tube, or more appropriately, the differential pressure transducer was difficult to calibrate. Dwyer gave two currents: 4mA for 0 in of water and 24 mA for 5 in of water. The easiest method for verifying these numbers would have been to place the planes inside one of Virginia Tech's wind tunnel facilities. However, this presented problems associated with mounting the planes to recorded accurate readings. Because of this, the numbers given by Dwyer have yet to be verified as of May 2003. The slopes were given in psf/Volt and the intercepts in psf. Error for the pressure readings was assumed to be on the order of several miles per hour.

4.4.4 Potentiometer Calibration

The throttle and elevon potentiometers were calibrated by selecting two points and measuring the corresponding rotation. The two points for the throttle were the minimum, 0, and the maximum, 1, settings given as a fraction of the total available throttle. The two points for the elevons were 0 deg and 10 deg. Because of errors associated with the potentiometer as well as the nonlinearities introduced by voltage divider circuits in general, the potentiometers circuits were assumed to have an error of ± 0.05 and ± 1 deg for the throttle and elevons respectively.

It is important to note that those instruments that could be calibrated were in fact tested both before and after the flight tests. This was particularly true of the potentiometer circuits. The accelerometer was found to be fairly consistent over time and so multiple checks proved unnecessary. This was undoubtedly due to the quality of the accelerometer construction and signal conditioning which was inherent in the cost relative to the other instruments. The flight test results recorded by this and the other instruments are given in Chapter 5.

Chapter 5

Flight Testing

5.1 Summary of Flights

Due to bad weather conditions, the first flight of the Delta Vortex did not occur until December 17, 2002. The Delta Vortex was not instrumented for this flight so the pilot could see how the plane flew before putting the expensive instrumentation array on it. The pilot commented that the plane was a "bit touchy" at first, but once trimmed properly the Delta Vortex became easy to control.

After implementing the instrumentation into the Delta Vortex (and with the building of the BetaMax under way) the first instrumented flight took place on March 14, 2003. The flight went very well and without any mishaps. The instruments worked well and the team was able to take data from all of them. The only unforseen problem that the team ran into was that the accelerometer data was aliased. This was due to the combination of the engine vibration (as much as 9000 RPM) and the low sample rate (20 Hz), and was later corrected with a second order low-pass filter for each axis.

After many weeks of building the BetaMax was finally completed and ready for its first trial flight on April 13, 2003. On this day the team also flew the Delta Vortex, and both

had instrumentation attached. The Delta Vortex flew as expected; however, a mishap with the accelerometer connection left the team without acceleration data for a second time. After the Delta Vortex landed and the instruments were relocated to the BetaMax, the BetaMax attempted its first flight with wings fully extended for maximum lift. It was not even able to lift off the ground and sustained minor damage after tumbling off the end of the runway. This was a major setback and the team began the difficult task of determining what went wrong.

The team found a couple major factors on why the BetaMax's failed to takeoff. It was apparent that it was having trouble rotating during takeoff. This was attributable to two things: center of gravity location and elevon size. As it turns out, the center of gravity was actually placed in the wrong location at the Delta Vortex specified location of 16.25 inches aft of the apex. After realizing this, the center of gravity was relocated to the precalculated correct distance of 16.25 inches to give the desired 10% static stability for the fully extended wing configuration, see Section 2.3.3. The second factor had to do with the fact that the elevons had been reduced in size by 25% after the wingspan was shortened. The elevons were therefore subsequently extended both outward to the wingtips and back to give roughly the same control surface area as the elevons on the Delta Vortex.

The first successful flight of the BetaMax, along with yet another flight of the Delta Vortex, occurred on April 19, 2003. With the telescoping wings partially extended, Beta-Max cruised down the runway and into the air. Not only did the BetaMax takeoff but it also extended and retracted its wings while flying. The pilot commented that it was very maneuverable with a tendancy to pitch up for the wings retracted configuration and very stable for the wings extended configuration. After 7 minutes of flight the BetaMax landed an sustained minor damage when the prop struck the runway.

Of course, as this was the first flight of the BetaMax, the team was more concerned with taking off, flying, and landing the aircraft in one piece and not so much in recorded

Figure 5.1: BetaMax flyover with wings fully extended

meaningful comparison data. The data presented in the following sections is therefore intended only to demonstrate the team's ability to record real-time flight test data. Data for comparison will hopefully be collected at a later date either by the 2002-2003 team or by the 2003-2004 team.

As a first case, the entire time histories are presented in Figures 5.3 and 5.2. The eight quantities presented are the roll rate, p (deg/s), the pitch rate, q (deg/s), the axial acceleration, a_x, the normal acceleration, a_z (g), the velocity, V (mph), the throttle position, δ_t, and the elevon positions, δ_e (deg). Note that the elevons are given on the same plot with the right elevon in blue and the left elevon in red.

It is clear from both sets of data that analyzing a 400-600 second complete time history of performance data can be overwhelming. This is especially true in this case where no particular flight plan was followed. Despite this fact, the team was able to locate a few instances on video of both planes performing certain maneuvers and link those instances with the corresponding flight test data. The following sections detail the results of these cases.

Two cases were investigated for the Delta Vortex: a vertical climb, and a loop and

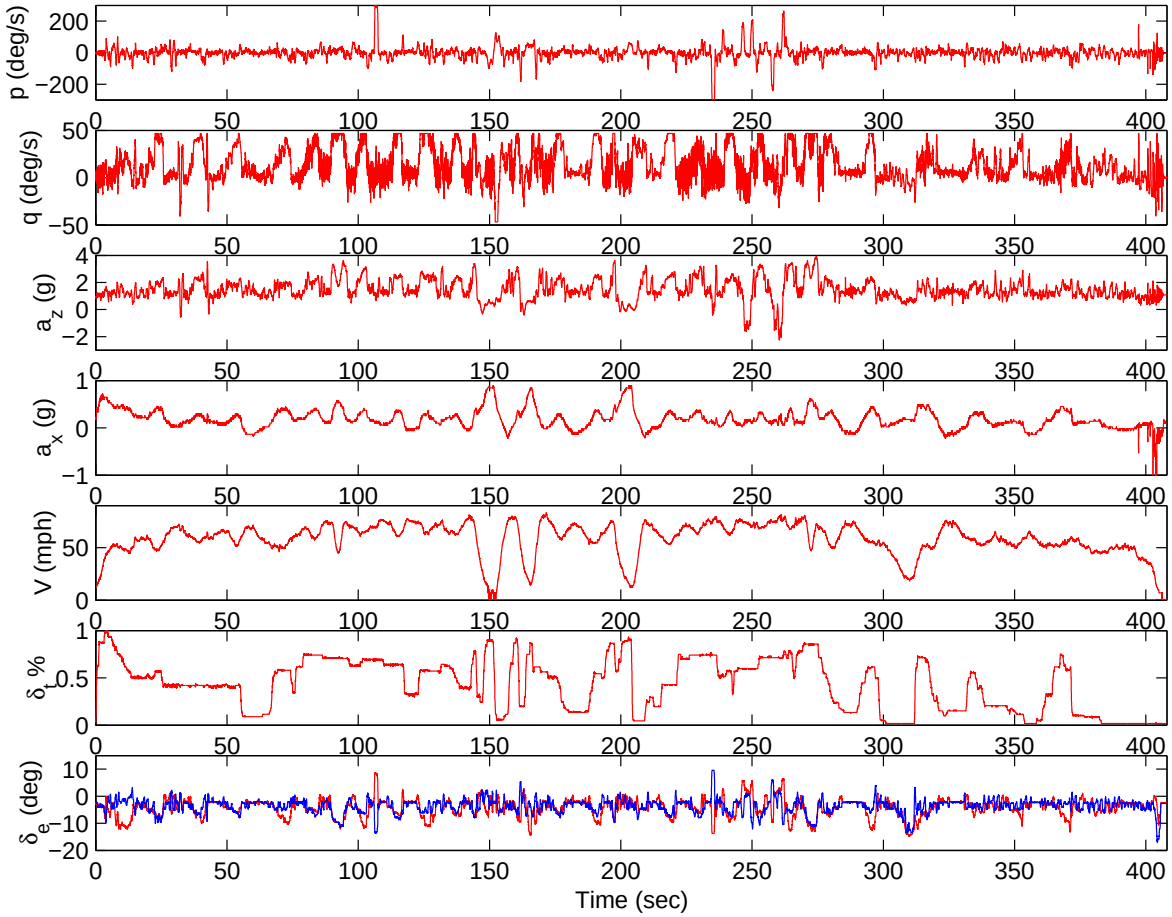

Figure 5.2: Delta Vortex complete time history

barrel roll. A single case was investigated for the BetaMax: a section containing a roll followed by the wing extension. For each of these cases, only six of the eight quantities are given. These include the roll rate, p (deg/s), the pitch rate, q (deg/s), the normal acceleration, a_z (g), the velocity, V (mph), and the elevon positions, δ_e (deg). The throttle and axial acceleration were shown to vary very little during these maneuvers are were therefore left out for this analysis.

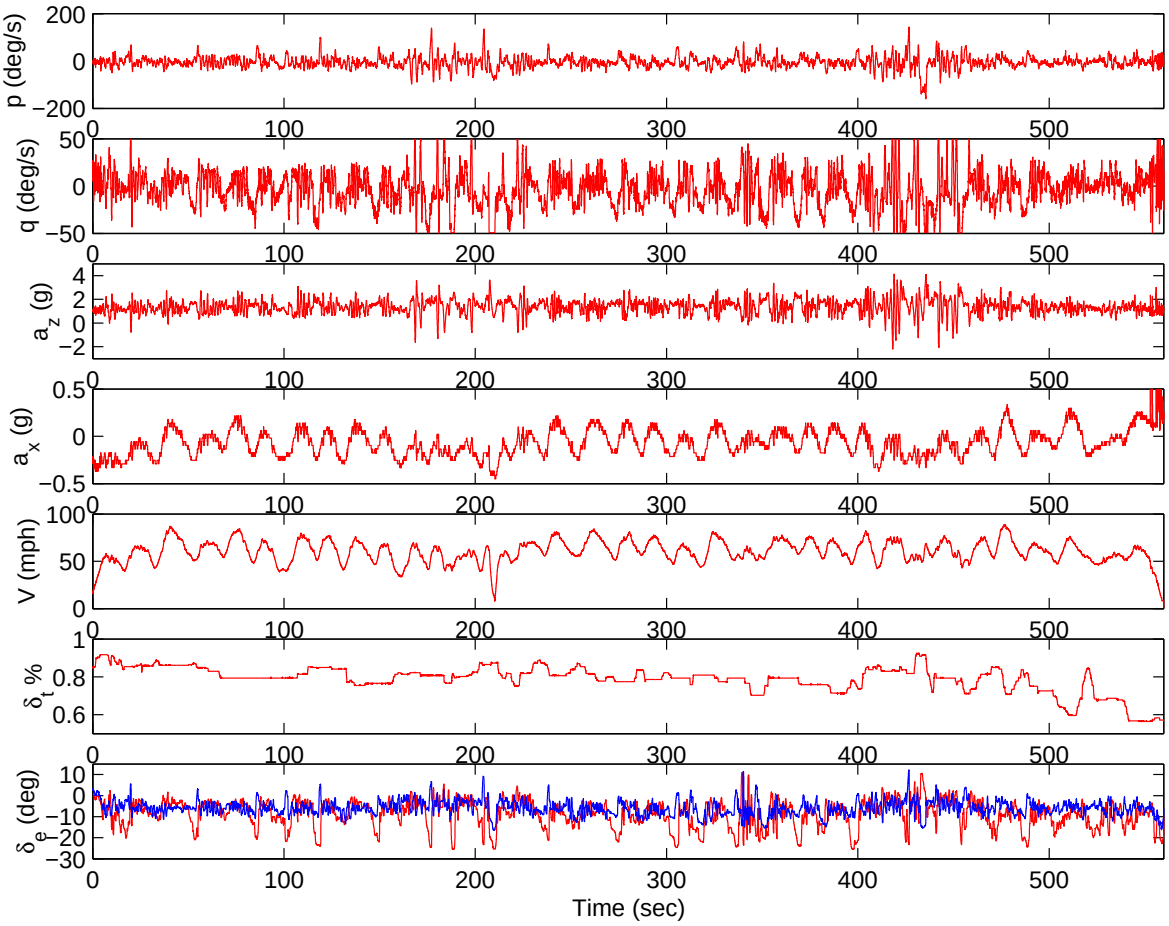

Figure 5.3: BetaMax complete time history

5.2 Delta Vortex Vertical Climb

The vertical climb case for the Delta Vortex took place around 190 seconds into the flight, see Figure 5.3. The 27 seconds of data for this maneuver is reproduced in Figure 5.4.

The maneuver begins with a bank which is evident from the differential elevon deflection and resulting roll rate around 1.5 seconds. At this point, the aircraft begins a turn pulling close to 2.5 g and exceeding the 50 deg/s pitch rate limit of the angular rate sensor. Throughtout this bank, the elevons can been seen to work both in unison as an elevator to make the turn and differentially to maintain the proper degree of bank. The turn is completed around 6 seconds as shown by the return of the normal acceleration to the 1 g

equilibrium condition.

The maneuver into the vertical climb begins at 8.5 seconds as is evident by the large negative deflection of the elevons and the subsequent rapid increase in pitch rate and normal acceleration. The vertical climb itself is shown to begin as the normal acceleration drops to 0 g around 12 seconds. At this point, gravity is no longer acting along the normal axis.

Based on the velocity data, the aircraft reaches its peak around 17 seconds. One might also infer from this data that the aircraft is in fact losing airspeed rapidly due to the vertical climb. However, looking at the throttle in Figure 5.3 at 205 seconds, it is clear that much of the drop in airspeed is attributable to the fact that the throttle had been cut. After talking with the pilot it was learned that this was done in attempt to stall the aircraft. Otherwise, the aircraft could have continued the climb for a much longer period of time.

Immediately after the aircraft reaches its peak, it begins to yaw (shown by the video) out of the climb into a steep dive. This fact indicates the possible presence of large sideslip angle (larger than the 15 deg limit set by Dwyer) and therefore an inaccurate reading in the Pitot-static reading used to calculate the velocity. The aircraft pulls out of the dive around 23.5 seconds as the normal acceleration levels back off around 1 g.

5.3 Delta Vortex Loop and Roll

The loop and roll maneuver takes place around 85 seconds into the flight. The time histories are given in Figure 5.5. This particular case is easier to visualize graphically than the vertical climb. The data can be easily separated by the two distinct maneuvers.

The loop begins around 3.5 sec and ends around 10.5 seconds. The pitch rate shows the fairly constant rotation of the aircraft (although it has clearly hit the maximum 50-deg/s limit). The normal acceleration also shows this; however, the ever constant change in orientation with respect to the gravity vector cause the equilibrium of the normal acceleration

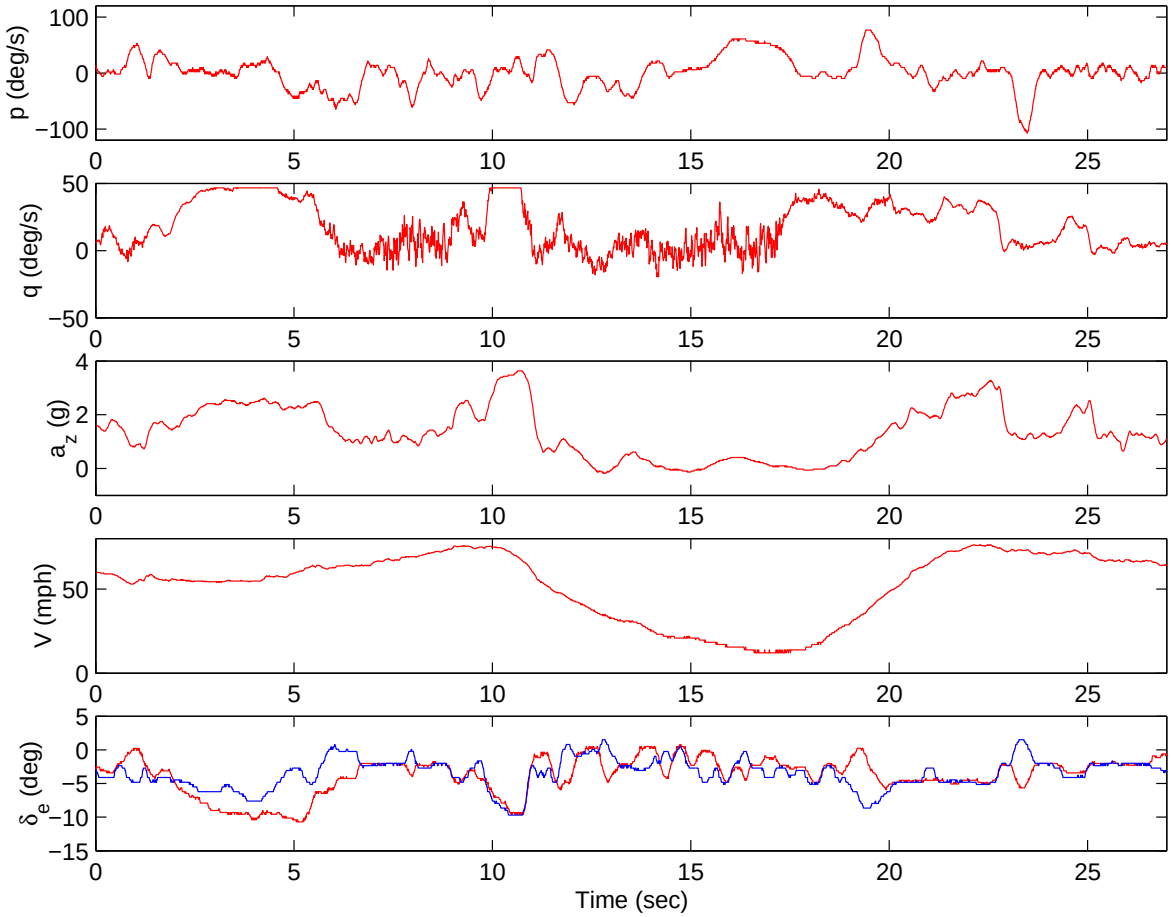

Figure 5.4: Delta Vortex vertical climb time history

data to shift from 1 g at the bottom of the loop to 0 g on either side and -1 g at the height of the loop. This of course is what indicates that this is a loop and not just a simple pull-up maneuver. The velocity time history is in agreement with this observation as the velocity reaches a minimum at the height of the loop. Of course, the angle of attack at this point is undoubtedly large enough (greater than the 15 deg limit set by Dwyer) to cause some inaccuracies in the Pitot tube readings.

Several seconds following the loop the aircraft banks and goes into at 2.5-3 g turn. At 20 sec, a barrel roll is performed. The large differential deflection and subsequent saturation of the roll rate sensor indicates a demanding command and an otherwise quick response (360

deg within 1.5 sec). This in itself however is of little use without something to compare results. That is, such maneuvers, while fast for manned aircraft, may be the norm for RC model aircraft. Having said that, it is important not to make any rash conclusions based on data from one of these aircraft.

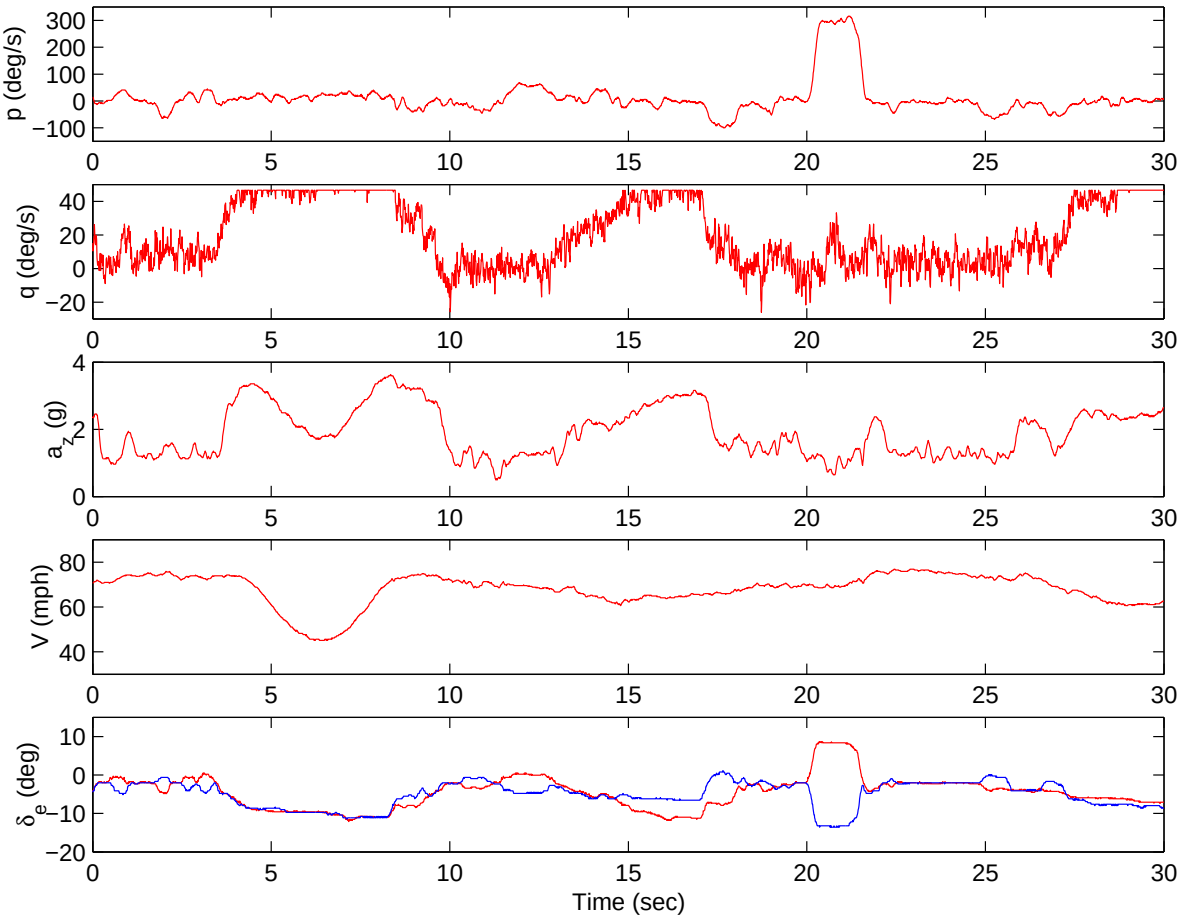

Figure 5.5: Delta Vortex loop and roll time history

5.4 BetaMax Roll and Wing Extension

The data presented here for the BetaMax is not really suited for comparison to the data extracted from the Delta Vortex. Because this was the BetaMax's first flight, caution was taken throughout the flight and no specific flight patterns were followed. The roll and wing

extension is seen in Figure 5.2 around 430 seconds. The 43-second maneuver is reproduced in Figure 5.6.

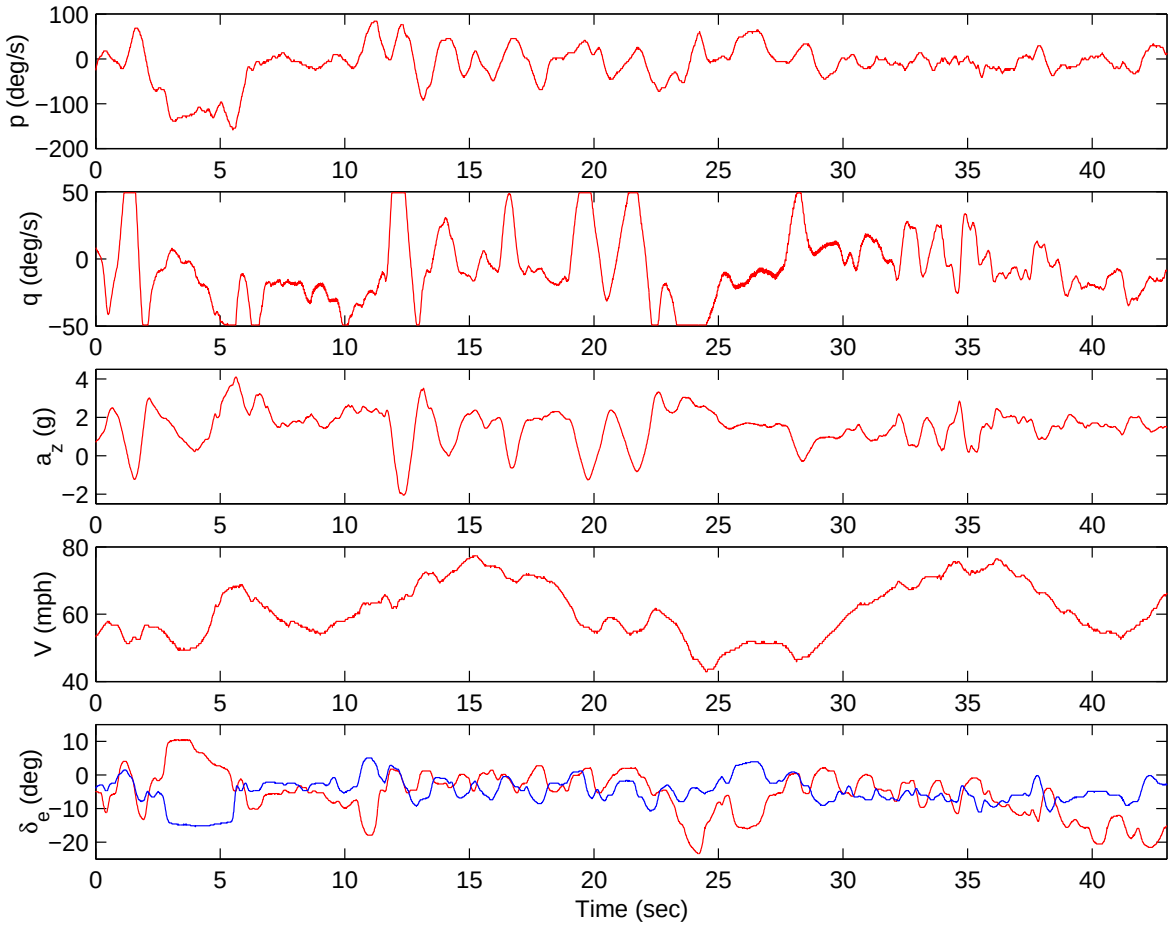

Figure 5.6: BetaMax roll and wing extension time history

The roll begins around 2.5 seconds as shown by the differential elevon deflection and -150 deg/s roll rate. An attempt could be made to compare this maneuver with the barrel roll of the Delta Vortex. However, the conditions would have to be analyzed in depth and the parameters normalized to extract a meaningfuly comparison. Suffice it to say that the BetaMax roll maneuver shown in Figure 5.6 took more than twice as long as the Delta Vortex roll maneuver for the same elevon deflection. Of course, this was partly a result of the BetaMax's lower airspeed, a speed nearly 20 mph less than that of the Delta Vortex.

Based on the video, the wing extension begins around 33 seconds. At this point, the pitch rate and normal acceleration show slight oscillations about the equilibrium. This is undoubtedly a result of the pilot corrections evident in the elevon deflections. After speaking with the pilot, it was determined that these minor corrections were necessary to stabilize the aircraft during the transition from the retracted to extended wing configuration. After the wings were fully extended (36 seconds), these oscillations are shown to die down considerably. This is true even at 38 seconds when a large differential deflection of the elevons is shown. This indicates the presence of a more stable configuration as expected. Again, the difference in static stability between the retracted and extended case was nearly 5%, see Section 2.3.3.

Chapter 6

Conclusions

The request for proposal (RFP) of this year's Virginia Tech AE/ME Morphing Wing design team was to design a full flying delta wing with morphing capability to provide a comparison to a conventionally controlled full flying delta wing aircraft. The project was undoubtedly a success.

A conventionally flying delta wing, The Delta Vortex, a product of Bruce Thorpe Engineering, was built by the team in the fall semester of 2002. Throughout the course of spring semester 2003, the team instrumented and flew The Delta Vortex to obtain flight characteristics relative to the performance of the aircraft. The spring semester of 2003 was also the beginning work with BetaMax. A design was conceptualized using the existing Delta Vortex and a unique morphing mechanism was devised to telescope the wings. BetaMax was then built and instrumented just like The Delta Vortex, and flown to obtain the same flight performance characteristics.

The two planes have not flown on the same day using the same flight plan so a direct comparison of performance data cannot be made at this time. The Delta Vortex and BetaMax are both ready to fly again when weather and time permits. At this point the data collected should be analyzed and compared to each other to obtain the desired comparisons

such a fuel efficiency, which directly correlates to range, roll rates and pitch rates during particular maneuvers, velocity at take off, etc.

The design team has laid an excellent foundation for any further work in this field. An instrumentation system has been implemented and proven to work, two planes have been built and are ready to be flown, and data has been collected from both planes. The data collected from each plane was not compared to one another, but each plane's data gives an idea of what type of characteristics the planes already have. Future research could include but is not limited to the collection of data from similar flight paths of many types, analysis of data to gather time to roll to 90 deg, 180 deg , and 360 deg, climb rates, short period damping, and natural frequency.

The 2002-2003 Virginia Tech AE/ME Morphing design team has designed, built, and flown a conventionally controlled full flying delta wing, and a delta wing with morphing capability. Instruments were purchased, calibrated, and implemented, and data was collected from each plane. Comparison of similar data from each of the planes should be analyzed in future research.

Appendix A

2002-2003 Budget

One of the main drivers and limiting factors of the Morphing Wing design project was the budget. The budget is a strong consideration when determining every factor involved in any design process. Accomplishing the goals set forth for the duration of the year will rely heavily on utilizing the budget provided to the team. Throughout the design process there will be opportunities available to increase the budget and raise additional funds, however the preliminary stages of the design process are highly restrained by funds the team has available.

The original budget for the 2 semester project was $5000. However, this is more of a goal, than a set amount of money. The total budget was never fully defined, and will remain dynamic throughout the project. The original funding was provided by the Center for Intelligent Material Systems and Structures, as well as the Mechanical Engineering Department of Virginia Tech. Throughout the course of the project, the team may also encounter opportunities to obtain additional funding from sources not affiliated with the university. The project began with little emphasis on keeping costs down.

A.1 Delta Vortex and Instrumentation Cost Considerations

The first goal of the semester was to build the model Delta Vortex RC aircraft. Emphasis was placed on required features of the kit, mainly size, rather than cost. The delta model aircraft that were considered ranged in cost from 53 to 200 dollars. The accessories for each plane would amount to the same cost regardless of the kit, so therefore the decision was based solely on the desired aspects of the kit and not the cost. The final decision (see Section 4.2) was to purchase the 54" wingspan Delta Vortex and a simulation program for a total cost of $148.00.

After the kit was purchased many accessories were needed to complete the construction and prepare the kit for flight. These accessories included engines, engine mounts, building supplies, and MonoKote skin material. The complete list of Delta Vortex Supplies can be seen in Table A.1.

The budget became limiting when considerations where made for the instrumentation (see Section 4.2). Instrumentation was extremely important in accomplishing the goals of this project. Without accurate instrumentation the comparisons made between the Delta Vortex and the Morphing RC plane would be useless, therefore finding the most effective instrumentation at the lowest cost was vital. To obtain accurate instruments while keeping total costs down, the list of desired instruments had to be limited. The search for instrumentation was greatly limited by the cost of the data logger, which is the most expensive of the instrumentation. Without a data logger that was reliable and compatible with all of the instruments, the data could not be analyzed. The final choice of data logger was one manufactured by Crossbow for a cost slightly under $1000. This was a good choice because it was small, light, and compatible with many instruments. The same was true for the process of choosing the individual instruments. Cheaper alternatives were also analyzed to determine

where corners should be cut concerning costs. The final price for chosen instrumentation was frugal, yet it produced a fully operative system capable of providing the desired data. The total cost of the final instrumentation system was $1,495.00. The summary of the instruments purchased and individual costs can be seen in Table A.2.

A.2 BetaMax Cost Considerations

The building of the BetaMax was extremely cost efficient which allowed for attention to detail. The costs of the Morphing Wing Delta aircraft were greatly minimized due to the supplies that were already purchased for the Delta Vortex. The morphing aircraft began with the identical kit used for the Delta Vortex. From there design alterations were made, and the kit was altered. Additional costs for the morphing aircraft included the costs of materials for the telescoping wings, and the mechanisms to operate them. Materials and supplies that were left over from the building of the Delta Vortex were utilized, which again kept second semester costs down. Additional structural materials were used but did not need to be purchased.

One consideration when choosing the instrumentation system was thoughts of the construction and testing of the morphing RC plane that was built second semester. The instrumentation already purchased was removed from the Delta Vortex and implemented on BetaMax. This was beneficial because two systems did not have to be purchased, minimizing costs. Reusing the system also allowed for more money to be spent on the instrumentation system resulting in more accurate and reliable instruments.

Few additional instruments were purchased, such as a pitot-static tube which would not be transferred from one plane to the other. There were also many materials used in the design and testing of the morphing surfaces of the aircraft there were never implemented on the final aircraft. These included materials to design and test the morphing trailing edge

control surfaces, and skins for them, even though this feature of the plane was dropped from the design late in the design process.

The Morphing wing project is a continuing project, so considerations were also made for the budget for the 2003/2004 project. The work accomplished in the first two years of the project has proven to be attractive to organizations outside of the university. Continuing interest from organizations such as DARPA and the Virginia Tech Center for Intelligent Material Systems and Structures will help to fund the project in coming years and help to continue making advancements on the current project.

Funding for the ME/AE Morphing Wing Team was a very important project driver throughout the 2002-2003 year. The budget will be a constant limiting factor as the project progresses trough years to come. Creativity in design and material selection will be vital in order to accomplish the goals of the ME/AE Morphing Wing Team that have been set forth with the money available to do so.

Table A.1: Delta Vortex Expenses

Item	Price	Quantity	Total
Delta vortex R/C Plane Kit	$88.50	1	$88.50
Simulator	$59.50	1	$59.50
Fox R/C Long Glow Plug	$2.49	3	$7.47
Pacer Zap CA 2 oz	$8.99	1	$8.99
Pacer Zap-A-Gap CA+ 1/2 oz	$2.99	1	$2.99
Tower Hobbies 6-Minute Epoxy 9 oz	$7.99	1	$7.99
Tower Hobbies 30-Minute Epoxy 9 oz	$7.99	1	$7.99
Top Flite MonoKote Transparent Orange 6'	$11.99	1	$11.99
Top Flite MonoKote Maroon 6'	$10.99	1	$10.99
Top Flite MonoKote Clear 6'	$11.99	1	$11.99
Great Planes Adjustable Engine Mount .60-1.20	$5.99	1	$5.99
Dubro Motor Mount .75 1.08 2-Stroke	$29.99	1	$29.99
Dubro S16 16 oz Square Fuel Tank	$4.49	1	$4.49
"Dubro Treaded Lite Wheels 3" "(2)"	$8.59	2	$17.18
"Dubro 3" " Spinner White"	$6.79	1	$6.79
Hitec HS-5645MG Torque Metal Gear Servo J	$54.99	5	$274.95
Hitec HS-5625MG Speed Metal Gear Servo J	$54.99	1	$54.99
Hitec Super Slim 8-Channel FM Receiver J	$59.99	1	$59.99
Hobbico HydriMax Panasonic 6.0V 2000 4/5A Flat U	$31.99	1	$31.99
Hobbico R/C Multi-Charger	$32.99	1	$32.99
Great Planes Filling Station Can Fitting Set	$4.69	1	$4.69
Tower Hobbies Tower Power 15% Fuel 4 Gallons	$57.00	1	$57.00
Top Flite MonoKote Jet White 7'	$10.99	1	$10.99
6677211 RX CRYL AM/FM 11 72010	$10.99	1	$10.99
Miscellaneous expenses since 10/11			$200.00
Total Delta Vortex Expenses			$1,021.42

Table A.2: Instrumentation Expenses

Item	Total
Dwyer Pitot tube (x2) and pressure transducer	$215.00
Analog Devices angular rate sensors (x2)	$120.00
Crossbow Data Logger	$960.00
Electrical Supplies	$200.00
Total Projected Instrumental Expenses	$1,495.00

Appendix B

Results of Controls Morphing

The original idea for the 2002-2003 morphing wing project was to change the shape of the trailing edge of our model to control it in flight. The hope was that the modified airplane with the morphing trailing edge would be more efficient and require less deflection than would be needed for a similar airplane using discrete control surfaces. The intended to prove that the control morphing airplane would have reduced drag and be able to execute maneuvers more quickly.

The 2001-2002 team experimented with somewhat less feasible ideas. Their use of piezoelectric and shape memory alloy actuated morphing systems served as valuable experimentation in the design process of the 2002-2003 team. After some deliberation, it was decided that a servo driven morphing section was the best choice.

This morphing section was to be accomplished by the use of two chord wise moving sections on the trailing edge of each rib. In the original design, these sections would be actuated by one servo with two rods attached. This configuration appears in Figure B.1.

During testing, this model failed. There was no limitation to the maximum deflection, if pushed too hard the rod and other parts would break. The trailing edge morphing sections were not stable. The thin material used for their construction was too flexible. When the

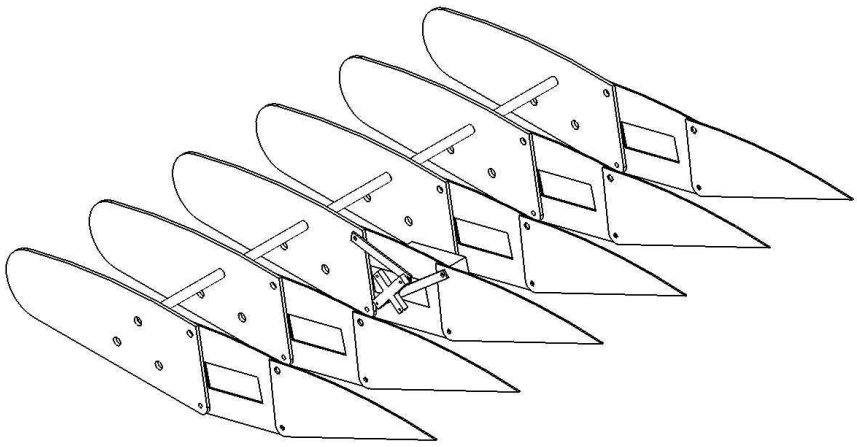

Figure B.1: Schematic of control morphing mechanism

latex skin was added to the outside and the mechanism was put in motion bending occurred. As the trailing edge moves from a fully deflected position to a non-deflected position the length from the tip to the tail is increased slightly. Instead of actually stretching the latex to the new length, the servo would bend the rib to the side to eliminate the extended length of the chord.

This mechanism was slightly modified to create better movement and more constrained deflection. The new mechanism shown schematically in Figure B.2 consisted of a stationary rib, a double plated moving middle section, and a fully moving trailing section. Due to the mechanisms design the trailing edge deflection was limited to 20 degrees, and the rigidity of the ribs was greatly increased.

The addition of skin to the mechanism was troublesome. The two considerations were that the skin material be stretchable and flexible. Latex fit both these conditions. When

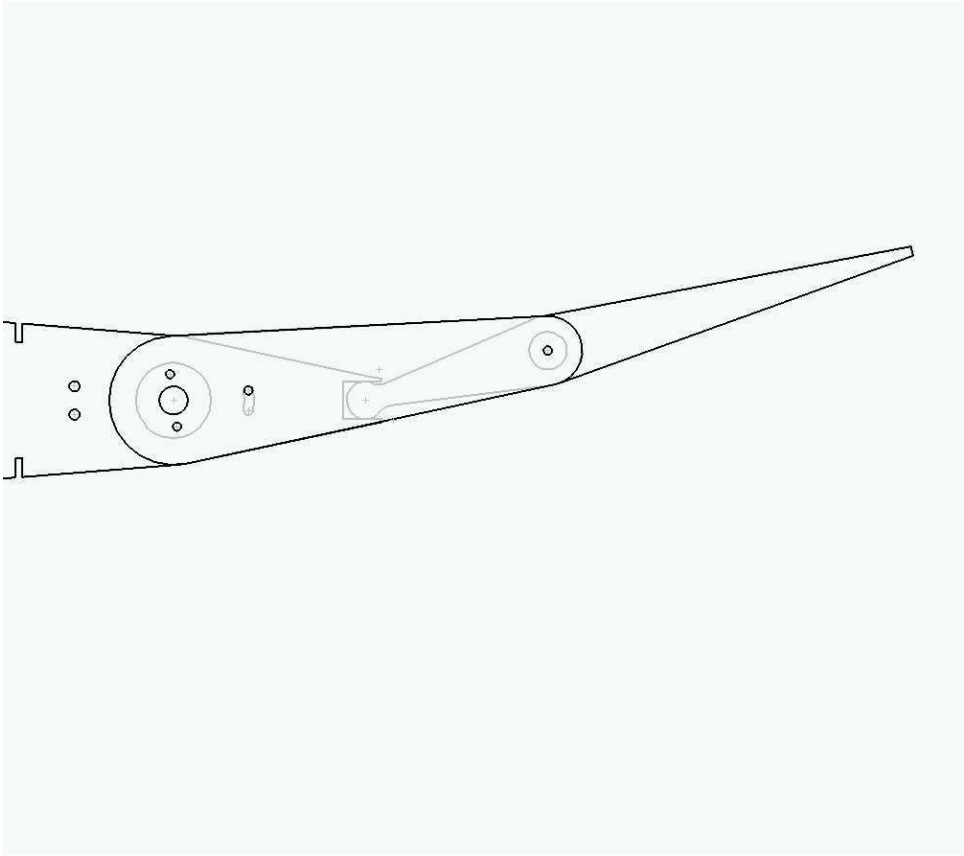

Figure B.2: Schematic of control morphing mechanism

latex was added to the mechanism considerable problems occurred. Rippling of the latex was the most prominent. If latex is not pulled with even force in all directions it forms ripples. These can be seen in Figure B.3. Since the latex is needed to stretch and release it could not simply be pre-stretched to the correct tension.

This problem was solved by using an inner layer of latex covered with a layer of Lycra. The Lycra chosen was only elastic in one direction. When this axis is laid parallel to the chord of the airplane, it reduces the rippling effect. This layered arrangement would satisfy all the requirements and alleviate most of the problems that arose with the use of latex.

Unfortunately due to circumstances beyond our control this design was put aside. The main piece of equipment used in making this mechanism was a Lasercam. This machine

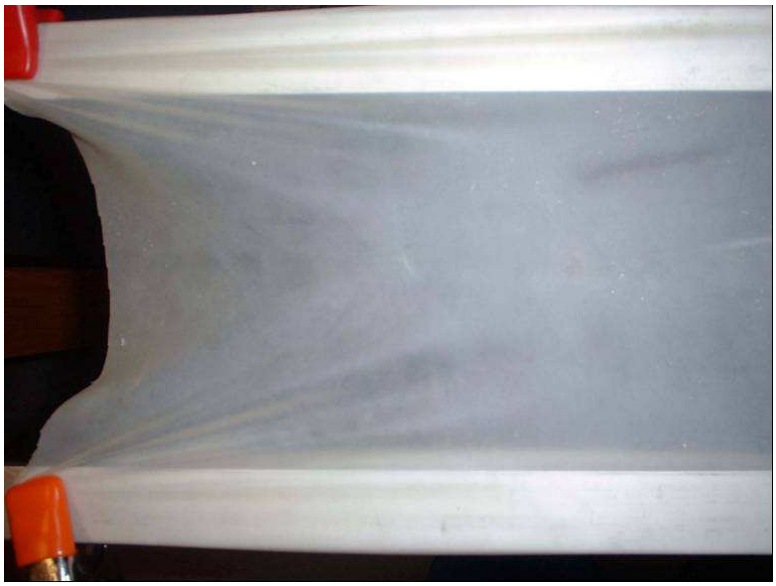

Figure B.3: Ripples in the Latex attached to the mechanism

would import shapes made in Mechanical Desktop and cut them out using a laser. During the critical building stage the machine was rendered inoperative. The machine's accuracy could not be duplicated by hand. With no definite timeline detailing its repair the team was forced to modify the projects mission statement. The new project would involve only morphing for mission diversity. A telescoping wing would be tested.

B.1 Skin Consideration

The skin of our aircraft is very important and needs to be chosen carefully. There are two main requirements it must fulfill. First, the skin must be flexible and stretchable. If the morphing aircraft is going to change shape, something that will move with it without affecting the aerodynamics of the vehicle is needed. The second requirement is that it be fairly resistant to the flow of air through it. We have several possibilities, each of which have problems. The first option is the use of Shape Memory Alloys. This would entail making the entire outer surface from a SMA. The problem with these is their response time. If the moving parts

were made of these materials, after deflection we would have to wait for the surface to cool down in order for them to move back. The next option is the use of Piezoelectrics. This idea, similarly to the SMA, would involve the use of sheets of piezoelectric material. The problem here is the constant supply of high voltage for a constant deflection. For trim conditions where a constant control deflection is needed it would drain batteries. Another option is the use of Integral Actuation. This idea involves laminated plies of fiberglass with embedded fibers of active materials arranged at 45 degrees to generate deflection and twist as needed. The problem here is the high cost and need for significant research and experimentation. The most feasible solution to the problem is the use of Latex/Silicon Rubber, or some other type of fabric that can be stretched. The problem in the past was that the servos were not strong enough to stretch the latex. This can be solved by finding a similar material with a lower modulus or by using servos that generate more power[2].

Appendix C

Output from Vortex Lattice Code VLM 4.997

A portion of the output file from the Vortex Lattice Method code VLM 4.997 is given below. The input data (reproduced in the output) is shown first. This data consists of coordinates (in inches) that define the wing's geometry. The important output is shown immediately after.

For the Delta Vortex, the VLM output was used to better approximate the aircraft neutral point, x_n, discussed in Section 2.3.3. The neutral point is determined from output parameter $\frac{C_m}{C_L}$ with the assumption that the center of gravity is at the nose of the aircraft ($x_n = 0$) and $C_{m0} = 0$. The equation relating C_m and C_L then is

$$C_m = C_{m0} + C_L(x_{cg} - x_n) \tag{C.1}$$

$$x_n = -\frac{C_m}{C_L} \tag{C.2}$$

Noting from the VLM output that $\frac{C_m}{C_L} = -17.09866$, the neutral point becomes $x_n = 17.09866$ inches. It is important to note that this is the distance from the leading edge of the wing to the neutral point in the specified dimensions (inches in this case). That is, the term $\frac{C_m}{C_L}$ is a dimensional term with units of the specified length. These units are specified when the input geometry file is created.

```
                              INPUT  DATA


         1. DELTA VORTEX: DELTA WING
         2.   1.       1.        1.0000     1336.5     0.
         3.  3.0
         4.  0.0         0.0      0.0       1.0
         5.  -24.5     -27.0      0.0       1.0
         6.  -37.0     -27.0      0.0       1.0
         7.  -37.0       0.0      0.0       1.0
         8. BASIC LINEAR AERO    20.  19.  0.25  0.55
         9.

.........

                     COMPLETE CONFIGURATION CHARACTERISTICS

         CL ALPHA         CL(TWIST)  ALPHA AT CL=0    Y CP      CM/CL       CMO
PER RADIAN   PER DEGREE
  2.68986     0.04695     0.00000     0.00000    -0.43183   -17.09866     0.00000

.........
```

Appendix D

Uncertainty Analysis

In order to determine the expected uncertainty and the associated error on calculated quantities, an uncertainty analysis is necessary. An iterative approach can then be taken to determine what kind of error is acceptable from measured quantities in order to be within the desired error limits on calculated quantities.

The uncertainty for a calculated quantity R can be determined as follows according to the measured quantities $a, b, c, ...$

$$R = f(a, b, c, ...) \tag{D.1}$$

$$\delta(R) = \sqrt{\left[\frac{\partial R}{\partial a}\delta(a)\right]^2 + \left[\frac{\partial R}{\partial b}\delta(b)\right]^2 + \left[\frac{\partial R}{\partial c}\delta(c)\right]^2 + ...} \tag{D.2}$$

The following sections detail the derivation of the uncertainty equations for lift coefficient and airspeed. In addition, a sample calculation is given with a specified reference flight condition. It is important to note that the "method of equal effects" was not used here as the error constraints on certain instruments would have been too great.

D.1 Uncertainty Equations for Lift Coefficient and Airspeed

By representing the lift coefficient, C_L, and airspeed, V, in terms of measured quantities, the relationships for each becomes

$$C_L \approx \frac{W n_n}{\bar{q} S} \tag{D.3}$$

$$V = \sqrt{2\bar{q}\frac{RT_{atm}}{P_{atm}}} \tag{D.4}$$

The uncertainties for each can then be found by applying equation D.2. The relations are

$$\begin{aligned} \delta(C_L) &= \sqrt{\left[\frac{\partial C_L}{\partial W}\delta(W)\right]^2 + \left[\frac{\partial C_L}{\partial n_n}\delta(n_n)\right]^2 + \left[\frac{\partial C_L}{\partial \bar{q}}\delta(\bar{q})\right]^2 + \left[\frac{\partial C_L}{\partial S}\delta(S)\right]^2} \\ \delta(C_L) &= \sqrt{\left[\frac{n_n}{\bar{q}S}\delta(W)\right]^2 + \left[\frac{W}{\bar{q}S}\delta(n_n)\right]^2 + \left[-\frac{W n_n}{\bar{q}^2 S}\delta(\bar{q})\right]^2 + \left[-\frac{W n_n}{\bar{q}S^2}\delta(S)\right]^2} \end{aligned} \tag{D.5}$$

$$\begin{aligned} \delta(V) &= \sqrt{\left[\frac{\partial V}{\partial \bar{q}}\delta(\bar{q})\right]^2 + \left[\frac{\partial V}{\partial T_{atm}}\delta(T_{atm})\right]^2 + \left[\frac{\partial V}{\partial P_{atm}}\delta(P_{atm})\right]^2} \\ \delta(V) &= \sqrt{\frac{P_{atm}}{8\bar{q}RT_{atm}}\left[\frac{2RT_{atm}}{P_{atm}}\delta(\bar{q})\right]^2 + \left[\frac{2\bar{q}R}{P_{atm}}\delta(T_{atm})\right]^2 + \left[\frac{2\bar{q}RT_{atm}}{P_{atm}^2}\delta(P_{atm})\right]^2} \end{aligned} \tag{D.6}$$

D.2 Sample Case: 66 fps at 2000 ft

A sample case was taken with 5% error for both the Pitot tube and the accelerometer. The reference condition considered was 66 fps at 2000 ft. Table D.1 shows the assumed values of the measured quantities and the associated assumed uncertainty.

Table D.1: Data for uncertainty sample at specified reference condition

Measured Quantity	Ref Value	Uncertainty
Dynamic Pressure, $\bar{q}$ (psf)	4.8	0.2
Atm Temperature, T_{atm} (R)	520	0.5
Atm Pressure, P_{atm} (psf)	1967	10
Weight, W (lb)	12	0.04
Normal Acceleration, n_n (g's)	2	0.1
Planform Area, S (sq ft)	9.55	0.2

The error for the lift coefficient, C_L, and airspeed, V, were found by substituting these quantities into Equations D.5 and D.6. Intermediate calculations for each are

$$\delta(C_L) = \sqrt{0.000003 + 0.000686 + 0.000686 + 0.0001203} \tag{D.7}$$

$$\delta(V) = \sqrt{2.722 + 0.001 + 0.028} \tag{D.8}$$

This gave a lift coefficient of $C_L = 0.52$, a lift coefficient uncertainty of $\delta(C_L) = 0.039$, and a total error 7.4%. Similarly, this gave an airspeed of $V = 66$ fps, an airspeed uncertainty of $\delta(V) = 1.7$ fps, and a total error of 2.3%. Section 4.2 discusses the significance of these results in more detail.

Bibliography

[1] http://www.flyg.kth.se/divisions/aero/software/tornado.

[2] http://www.intellimat.com/materials/applications/active-helicopter-rotor-blades.html.

[3] Defense Advanced Research Project Agency. BAA 01-42, Addendum 7, Special Focus Area: Morphing Aerialaircraft Structures (MAS). http://www.darpa.mil/baa/baa01-42mod8.htm, September 2001.

[4] Kenneth L. Bonnema and Stephen B. Smith. AFTI/F-111 Mission Adaptive Wing Flight Research Program. pages 155–161, San Diego, California, 1988.

[5] Greg Eggleston et al. Morphing Aircraft Design Team. http://www.aoe.vt.edu/mason/Masonf/FinalMorphRpt02.pdf, May 2002.

[6] Henry Ford Museum and Greenfield Village. The Wright Brothers. http://www.hfmgv.org/exhibits/wright/, July 1995.

[7] Federation of American Scientists. B-1B *Lancer*. http://www.fas.org/nuke/guide/usa/bomber/b-1b.htm, October 1999.

[8] Federation of American Scientists. F-14 *Tomcat*. http://www.fas.org/man/dod-101/sys/ac/f-14.htm, April 2000.

[9] Brian L. Stevens and Frank L. Lewis. *Aircraft Control and Simulation*. John Wiley and Sons, Inc., New York, 1992.

[10] J. R. Wilson. Active Aeroelastic Wing: A New/Old Twist On Flight. *Aerospace America*, 40(9):34–37, September 2002.